

1 *Response file on “Debris flow modeling at Meretschibach and Bondasca catchments,*
2 **Switzerland: sensitivity testing of field data-based erosion model”** by F. Frank, B.W. McArdell,
3 N. Oggier, P. Baer, M. Christen and A. Vieli
4 florian.frank@wsl.ch

5 **Reviewer 1:** Z. Han

6 **Reviewer 2:** Anonymous

7 **Editor:** M. Keiler

8 **(A) Comments from referees/public**

9 **(B) Authors response**

10 **(C) Authors changes**

11 **General comment by the authors**

12 In addition to the comments from the Editor and Reviewers, a few additional minor changes to the
13 text have also been made for clarity. These changes are also visible in the document highlighting
14 the changes made to the manuscript. A few formal errors (e.g. typos, etc.) were also fixed.

15 **PLEASE NOTE:** The page/line(s) references provided by **(A) reviewers and editor** and **(B)**
16 **Response** still refer to first submission manuscript.

17 But all page/line(s) references given by the authors (“**(C) Changes**”) in this document refer to the
18 new resubmission manuscript (which highlights **track changes in RED** and **text moved in GREEN**).

19 **General comments by Reviewer 1**

20 **(A) Reviewer 1:** This paper aims to simulate debris-flow process by considering bed erosion along
21 the path. As erosion is a complex natural process and plays a very crucial role both in debris-flow
22 dynamics, transportation, run out and deposition process, it is a very important research topic. To
23 do so, this paper attempts to combine an empirical entrainment model which has been previously
24 introduced by authors into the RAMMS model. The sensitivity of the developed model is tested by
25 applying the model to two debris-flow events in Switzerland. The results show some interesting
26 erosion and flow patterns.

27 **(B) Response:** We are grateful for the thorough reading of the manuscript and the helpful review,
28 which we think will substantially improve the manuscript. We address both the general and specific
29 comments below.

30 **(C) Changes:** Please see further general comments of Reviewer 1 below and “Specific comments”.

31 **(A) Reviewer 1:** Generally, this is a straight-forward development of the RAMMS model for the
32 simulating bed erosion in debris flows. The paper is well illustrative and authoritative. The authors
33 build upon their previous work and extend the RAMMS model to the erosion simulation. It is a
34 major contribution and is sound. However, in my opinion, the major limitation of this paper is that
35 the described debris-flow entrainment model is rather sensitive to the empirical coefficients, and
36 these coefficients are not well illustrated in the paper. Indeed, the authors show us a sensitivity
37 analysis of erosion volume to the initial volume, erosion rate and calibrated parameters and in
38 Fig.7. As they mention, the value of these parameters are suggested by the previous study in the
39 same region, e.g., the erosion rate $dz/dt = 2.5$ cm/s. However, the rational range of these parameters
40 may be different in other regions, there is a need to explain how to determine these parameters. The
41 paper could be improved and made more accessible by further exploring these empirical
42 parameters. I recommend this paper for publication after major revisions.

43 **(B) Response:** Yes, we agree that the results of the model are quite sensitive to the empirical
44 coefficients and the initial conditions, which is the main focus of the manuscript. The uncertainties
45 in the field data (e.g. initial flow volume, volume of eroded sediment, magnitude of erosion) are
46 generally fairly large. It may be by chance that the same coefficients deliver plausible results at
47 three different debris-flow sites in the Swiss Alps when in fact it may be possible to refine the
48 coefficients in cases where more precise field data are available. For this reason, all of the
49 coefficients can be adjusted when more or better results become available. We intend to edit the
50 manuscript to make this point more clear. To further explore the influence of the parameter
51 combinations, we also intend to highlight the inherent feedback in the model, whereby a rapid
52 erosion rate results in an increase in flow depth leading to larger shear stresses and then to even
53 larger potential erosion depths. This potentially explains the very rapid growth of debris flows,
54 which is has been observed in some natural field cases and also in laboratory experiments
55 involving realistic debris-flow sediments (e.g. Logan & Iverson, 2007, Video documentation of
56 experiments at the USGS Debris-flow flume 1992-2006, U.S. Geological Survey Open-File Report
57 2007-1315).

58 **(C) Changes:** Editing of the manuscript was processed in sections 4.2. (page 12) and 5.
59 (discussion, starting at page 14) to make the points mentioned above more clear. The reference list
60 has been updated accordingly.

61 **General comments by Reviewer 2**

62 **(A) Reviewer 2:** The paper deals with bed entrainment for debris flows in Switzerland using
63 numerical modelling. The topic is of interest for the Journal and the specific issues of this paper are
64 relevant to scientists and practitioners. Some (mandatory) changes are required to improve the
65 paper before acceptance. The list of specific comments and suggestions is given in the attached file.

66 **(B) Response:** We are grateful for the helpful specific comments, especially literature citations
67 which were not cited in the last version of the manuscript. These comments should substantially
68 improve the manuscript. Please see our responses to the specific suggestions below.

69 **(C) Changes:** Please see “Specific comments”.

70 **Specific comments by Reviewer 1**

71 **(A) Reviewer 1: Page 6, 195-196.** The authors mention that the slope angle ϕ in the deceleration
72 term S_f is similar to the internal friction angle of the material. Does it mean that S_f will be the same
73 when at a steep slope and a gentle slope? Please check it.

74 **(B) Response:** Yes, it is true that the slope angle is similar to the angle of internal friction at this
75 slope. However we do not imply that the value of S_f in the Voellmy friction relation is the same as
76 the value of internal friction in general. We intend to remove this comment to avoid confusion for
77 readers, because the Voellmy friction angle is typically selected based on other criteria.

78 **(C) Changes:** The comment in parenthesis “(approximately similar to the internal friction angle of
79 the material)” was removed (page 8, lines 208-209).

80 **(A) Reviewer 1: Page 7, 221-222.** The critical shear stress τ_c determines the maximum potential
81 erosion depth e_m , the erosion will not be existed at the area where $\tau < \tau_c$. For this reason, the critical
82 shear stress is a key parameter for controlling the shape of erosion area and erosion depth. But the
83 authors superficially use an empirical value 1 kPa in the paper, and no sensitivity analysis is made.
84 It seems that they could simply test and provide results on how sensitive the simulation is to the
85 choice of the critical shear stress τ_c .

86 **(B) Response:** Yes, we did not include results for the sensitivity analysis regarding the value of the
87 critical shear stress, because the influence is generally much smaller and the range of critical shear
88 stress values is small. We disagree that our choice and use of 1 kPa is superficial, because this
89 value based on indirect observations by Schürch et al. (2011, cited in the original manuscript) and it
90 serves a general purpose of describing that torrent channel beds are typically not eroded by small
91 debris flows. We do not know the precise value in the field at any field site however a value near 1
92 gives a good fit to the data set we used for that analysis. Using a Shields’s criteria for critical shear
93 stress from river engineering, we find a critical shear stress which is smaller than 1, depending on
94 the grain size on the channel bed. We discussed the issue of different critical shear stresses in our
95 first erosion model application at the Spreitgraben catchment (Frank et al., 2015). Therein, we
96 described smaller debris flood events which produced about 4-5 kPa of shear stress but did not
97 show any significant erosion in the channel bed, i.e. suggesting that the critical shear stress τ_c may
98 be somewhat larger in the Spreitgraben than in the Illgraben channel.

99 We propose inserting a paragraph discussing this issue in more detail, especially noting that the
100 value is close to zero, or could be set to zero if field evidence indicates that erosion is always
101 expected. However we will gladly include such a plot as an additional figure if this is desired by
102 the editorial staff.

103 **(C) Changes:** We performed additional model runs to assess the sensitivity of the model results to
104 the critical shear stress value. We also changed the comparison from the *bulking factor* to *volume*
105 *growth* (Hungri et al., 2005). For this assessment, we selected the Meretschibach catchment because

106 it has a simple single-channel morphology channel geometry and therefore serves as a clear case
107 for illustration. The results are presented in the new Figure 8. The former Figure 8 is now Figure 9
108 - which we also updated to show results as volume growth instead of using the bulking factor BF.
109 The values for BF have all been recalculated as VG values and the manuscript has been updated
110 accordingly. We added a short description of the results in section 4.3 (pages 13/14, lines 402-
111 411)., introduced the VG equation (Eq. 8, moved to section 4.3, page 13, line 407), and now we
112 discuss the results as presented in Fig. 8 in a new paragraph in the middle of the discussion section
113 (page 16).

114 **(A) Reviewer 1: Page 11, 360.** The total erosion volume remains approximately constant when the
115 initial volume exceeds a certain value. How to explain this phenomenon? Is this because the
116 maximum erosion depth e_m is reached as controlled by the critical shear stress $\tau_c = 1$ kPa? As such,
117 it seems that the choice of τ_c as a model parameter should be discussed to a greater degree,
118 especially if you want your method to be used more widely on debris flows of varying properties.

119 **(B) Response:** In fact, the volume continues to increase (the y-axis is a logarithmic scale). The
120 maximum erosion depth e_m may be limiting – however e_m also increases due to increasing
121 maximum flow heights (see also Fig. 3 in Frank et al., 2015) when systematically enlarging the
122 initial release volumes in the sensitivity analysis. Again, the model is insensitive to the value of
123 critical shear stress once that value is exceeded (please refer to our comment above).

124 **(C) Changes:** See changes as described in the comment above. We added the new Figure 8
125 (sensitivity analysis for τ_c). Changes were made in section 4.3 to describe the data presented in the
126 new Figure 8 which we discuss in a new paragraph in the middle of our discussion (page 16).

127 **(A) Reviewer 1: Page 12, 396-397.** As I see in Fig.3, there is no significant difference of runout
128 distance in B2 ($\mu=0.6$) and B3 ($\mu=0.7$). Please check the sentence “ μ controls the runout distance”.

129 **(B) Response:** The sentence “ μ controls the runout distance” is consistent with the Voellmy
130 friction relation as used in runout models such as RAMMS. It is not a result from this present
131 study. We will provide a suitable literature citation for that statement and adjust the wording to
132 ensure that readers do not see this as a result of this project. Perhaps the problem lies in the
133 illustration of the modeling results for three μ values. The calculation domain, where the software
134 was used, was limited in spatial extent to the area where we have differential DTM data for
135 comparison (e.g. the blue polygon in Fig. 3A), so we actually do not show the final runout distance.
136 In the process of answering this comment, we noticed that the blue polygon is drawn inconsistently
137 in figure 3B1-B3, but it is drawn correctly in Fig. 3A. We will also correct this error in the final
138 manuscript.

139 **(C) Changes:** We now provide a literature citation “(Bartelt et al., 2013)” for the statement “ μ
140 controls the runout distance (page 14, line 429). We’ve also adjusted the wording in this paragraph
141 of the discussion chapter to ensure that readers do not see this as a result of this project (page 14,

142 lines 431-435). We also adapted the inconsistently drawn blue polygons in figure 3B1-B3 to be
143 consistent with the correctly drawn blue polygon in Fig. 3A.

144 **(A) Reviewer 1: Page 27, 675.** The total erosion volume in both cases show an abrupt decrease,
145 and then a significant increase with the initial release volume, i.e., 1-2 m³ in Meretschi and 10-20
146 m³ in Bondasca. Is there any rational explanation on it?

147 **(B) Response:** When comparing erosion depths as modeled using 10 vs. 20 m³ as the initial
148 volume in the Bondasca case e.g., we observed that the model run using 20 m³ is large enough that
149 part of the flow enters a secondary channel. The volume of the flow, then divided among two
150 channels, causes a reduction in flow depth and a consequent decrease in shear stress, resulting in
151 smaller erosion depths and therefore smaller erosion volumes. When using an initial volume of 10
152 m³ then the flow fully stays in the main channel. We propose adding a small discussion paragraph
153 explaining this issue.

154 **(C) Changes:** We added a brief discussion paragraph explaining this issue (page 17, lines 517-
155 525).

156

157 **Specific comments by Reviewer 2**

158 **(A) Reviewer 2: Page 1, lines 23-24.**

159 why this choice. Basal friction and bed entrainment are interplaying in natural processes. Why
160 separate calibration?

161 **(B) Response:** We decided to first calibrate the runout of the model based on the total volume of
162 the event and the runout distance, and then work with smaller initial volumes, then including the
163 erosion algorithm, to refine the results. Our goal was to avoid a time-intensive iterative procedure,
164 especially for the benefit of practitioners who generally do not have time to go through a long
165 calibration process. However the model could also be calibrated by starting with small landslide
166 volumes, so this is just a statement of how we performed the calibration.

167 **(C) Changes:** We added a few words at this location in the abstract section to further clarify this
168 (page 1, lines 24-27).

169 **(A) Reviewer 2: Page 2, line 34.**

170 you mean rheology?

171 **(B) Response:** This sentence would be better stated as follows: “Sediment erosion caused by debris
172 flows causes flow bulking (in our case an increase in flow mass; Iverson 1997) which strongly
173 influences the runout behavior of debris flows.” We suggest to change it to clarify this.

174 **(C) Changes:** We changed the first sentence of the “Introduction” chapter as suggested (page 3,
175 lines 39-41).

176 **(A) Reviewer 2: Page 2, line 38.**

177 quote also works of:

178 - Cascini et al. (2106) Eng Geol

179 - Cuomo et al. (2016) Eng Geol

180 - Cuomo et al., (2014) Canadian Geotechnical Journal

181 where bed entrainment is discussed as far as its spatial-temporal variation, and its interplay with
182 rheology

183 **(B) Response:** Thank you for pointing out this additional literature, which we did not initially
184 consider for this manuscript. However our focus is not on the rheology of the flow or changes in
185 the rheology as a consequence of entrainment. As stated in the manuscript, we use the Voellmy
186 friction relation and we do not adjust the Voellmy friction coefficients as a function of flow
187 properties. However we propose including this as a discussion point, where we will be able to cite
188 some of these publications.

189 **(C) Changes:** We added this as a short discussion point and cite some of the publications in the
190 paragraph which already described how morphological effects influence the erosional behavior of
191 the model (page 15, lines 462-466). The reference list has been updated accordingly.

192 (A) **Reviewer 2: Page 2, line 45.** what is this? bed entrainment? you may also call erosion. But
193 bulking process is hard to understand and not common in international literature.

194 (B) **Response:** The term “bulking” is commonly used in the literature to describe the increase in
195 mass of a debris flow along the flow path ,e.g. see Iverson, R. M.: The Physics of Debris Flows,
196 Reviews of Geophysics, 35, 245-296, 1997. doi: 10.1029/97RG00426, 1997, for a clear
197 explanation in a paper which is very widely cited by debris-flow and landslide researchers
198 throughout the world. A quick search on an academic search engine also indicates that “bulking” is
199 commonly used in the debris-flow literature by authors from many countries outside of
200 Switzerland, so we respectfully disagree with Reviewer 2 on this point. We realize that it may have
201 other meanings in other academic disciplines, so we propose that we clarify the terms like this in
202 the next version of the manuscript.

203 (C) **Changes:** Further clarification of the term *bulking* is made by "(in our case an increase in flow
204 mass, e.g. Iverson, 1997)" in the first sentence of the Introduction section (page 3, lines 39-41).
205 Additional definitions of the terms *erosion*, *entrainment* and *bulking* are given in the following
206 sentences (page 4, lines 41-45). Throughout the rest of the manuscript, we made sure that we use
207 those three defined terms consistently.

208 (A) **Reviewer 2: Page 2, line 55.**

209 is there any difference?

210 (B) **Response:** Erosion removes sediment from the channel bed, bulking describes the increase in
211 size (mass) of the flow, so the two terms are closely related but not interchangeable. As stated
212 above, we will, in the next version, provide definitions of the terms.

213 (C) **Changes:** These changes have been addressed in our response on line number 202 of this
214 document.

215 (A) **Reviewer 2: Page 2, lines 57-61.**

216 there are cases where neglecting erosion one may obtain unsafe future scenarios, as bed
217 entrainment change the propagation pattern, and thus influence the global behaviour of the
218 landslide. This is especially true for debris avalanches (not channelised). However, also for debris
219 flows, including the entrainment helps obtaining better model estimates. See, for instance Cascini
220 et al. 2014 Geomorphology

221 (B) **Response:** Thank you for pointing out this paper, which we will consider citing for the next
222 version of the paper. We agree that including entrainment may help users to obtain more accurate
223 predictions.

224 (C) **Changes:** We cited Cascini et al. (2014) in the introduction section (page 4, line 77) and the
225 reference list has been updated accordingly.

226 **(A) Reviewer 2: Page 2, lines 73-74.**

227 add models by Pastor et al.. You may find applications in previous works of Cuomo et al.

228 **(B) Response:** Thank you for pointing out these additional papers, which we will cite, if
229 appropriate, in for the next version of the manuscript.

230 **(C) Changes:** We cited Pastor et al. (2009) there (page 4, line 75) and the reference list has been
231 updated accordingly.

232 **(A) Reviewer 2: Page 2, lines 76-79. Also line 165 (which does not have a comment, just a
233 highlight).**

234 are you using erosion, entrainment and bulking with the same content?

235 **(B) Response:** It is not clear to us if this comment is about the terminology or the differences in the
236 bulk properties of the flow vs. the channel bed, so we will address both comments:

237 (1). In our case, the bulking (increase in mass of the flow) produced by entrainment (the process
238 described in the model which specifies how fast and where the additional sediment enters the
239 debris flow) should be clear (also see our comments above regarding terminology). Net
240 entrainment of sediment (erosion – deposition) results in net erosion of the channel bed (a decrease
241 in the elevation of the channel bed), which can then be characterized in a spatial sense with a
242 description of a pattern.

243 (2). Although it is possible to specify a different mass density for the sediment that is entrained
244 from the channel bed, to a first approximation the mass densities of the two are similar, at least in
245 torrents which experience frequent debris flows. In more detail, the degrees of sorting and ranges
246 of grain sizes in both the flow deposits and the channel bed are fairly similar. However the model
247 accounts for differing densities, if such values are available.

248 **(C) Changes:** These changes have been addressed in our response on line number 202 of this
249 document.

250 **(A) Reviewer 2: Page 6, line 192.**

251 turbulent factor. And, it is does not depend on v^2 . rephrase the whole sentence.

252 **(B) Response:** Thank you for pointing out that this is not clear to you, we propose that we re-write
253 the sentence in question.

254 **(C) Changes:** By revisiting the referenced RAMMS papers (Christen et al., 2010; Christen et al.,
255 2012; Bartelt et al., 2013), we re-wrote the entire sentence (page 7, line 202-206).

256 **(A) Reviewer 2: Page 7, line 220. ??**

257 **(B) Response:** Thank you for pointing out the error in the reference number of the equation, we
258 will fix that in the next version of the manuscript (it should be Eq. 6).

259 **(C) Changes:** Error fixed at page 8, line 234.

260 **(A) Reviewer 2: Page 7, line 221.**

261 from where this value? / from where?

262 **(B) Response:** These values were described by Frank et al. (2015), however upon re-reading the
263 paragraph above Equation 6, we realize that we should add more details in the next version of the
264 manuscript. Additionally, we propose adding “Frank et al. (2015)” at the end of the sentence to
265 make the origin more clear to the reader.

266 **(C) Changes:** We added the reference to our first entrainment model study “(Frank et al., 2015)”
267 (where all details can be found) at the end of the two sentences to make the origin of the values and
268 factors of the entrainment model more clear to the reader (page 8, line 232 and line 236). We also
269 added a few words in this paragraph to give more details (page 8, line 232-236).

270 **(A) Reviewer 2: Page 7, lines 229-230.**

271 check numbering of eqs

272 **(B) Response:** Thank you for pointing out the error in the reference to the equation, we will correct
273 and verify all equation numbers when preparing the next version of the manuscript.

274 **(C) Changes:** Error fixed at page 9, lines 243 and 244.

275 **(A) Reviewer 2: Page 9, line 281. -2.5 ?**

276 **(B) Response:** We agree with your suggestion we will also change the value to SI units, so -0.025
277 m/s, also for other occurrences of $\frac{dz}{dt}$ values in the manuscript.

278 **(C) Changes:** We changed the erosion rate values to SI units, so -0.025 m/s, for all other
279 occurrences of $\frac{dz}{dt}$ values in the manuscript.

280 **(A) Reviewer 2: Page 10, line 314.**

281 how this was fixed?

282 **(B) Response:** The parameter ξ was determined by varying it within the range proposed by the
283 developers of the RAMMS model ($\xi = 100, 200, 400$) and inspecting the results. The only realistic
284 velocities (in the steep ($\approx 60\%$) study reach of the Meretschibach channel) are obtained using $\xi =$
285 200 when combined with the variation of parameter μ ($= 0.5, 0.6, 0.7$). This is explained in the
286 manuscript on page 10, lines 312-316. However to ensure that this is clear, we propose adding a
287 sentence to clarify this procedure.

288 **(C) Changes:** We added a sentence (page 11, lines 331-333) to clarify the calibration and model
289 set up procedure. We also updated the previous sentence in the manuscript (page 11, lines 327-329)
290 to eliminate an inconsistency in how the model was actually applied in this case (e.g. it was
291 correctly described in section 3.3.2. (page 10, lines 288-292) and in the caption of Fig. 6 on page
292 30, lines 794-797).

293 **(A) Reviewer 2: Page 13, line 432.**

294 Alternative, but related definition is that of Hungr, i.e. landslide growth rate = $V_{\text{final}} / V_{\text{initial}}$

295 **(B) Response:** Thank you for pointing out Hungr's definition. We will verify which metric are
296 used in the other papers which we reference, and for the next version of the manuscript we will
297 choose the most suitable metric (as well as cite Hungr's landslide growth factor).

298 **(C) Changes:** We followed your suggestion for an alternative definition of the metrics and we now
299 use Hungr's *volume growth* (VG) instead of the *bulking factor* (BF) (pages 13-14, lines 402-411
300 and new Figure 8). The VG values in the text were adjusted accordingly to Figure 9 (formerly
301 Figure 8). However this change has not changed the interpretation of the results or the discussion
302 thereof (pages 16-17).

303 **Comments by the Editor (referencing comments from Reviewer 1 and 2)**

304 **(A) Editor: Reviewer 1, general comment:** additionally, provide also a short review on
305 theoretical concepts explaining this behavior and how it is related to your model

306 **(B) Response and (C) Changes:** As mentioned above in the response to the general comments by
307 reviewer 1, we edited sections 4.2. (calibration, on pages 11 and 12) and 5. (discussion, starting at
308 page 14) for clarity . In section 5 we also added a discussion about the inherent feedback of in our
309 entrainment model and its relation to the similar observations in laboratory and field studies (page
310 17, lines 535-541). We added several new comments and references to related discussions in our
311 previous manuscript where the model was introduced (Frank et al., 2015). Recent entrainment
312 modeling papers (e.g. Cuomo et al., 2016) are now referenced (page 15, line 463) and discussed in
313 relation to our empirical approach (these references were suggested in some specific comments by
314 reviewer 2).

315 **(A) Editor: Reviewer 1: Page 6, 195-196.:** I think just deleting the sentence is not a good solution.
316 You have to explain your choice for the parameter of internal friction, It seems that you did not
317 used the typical criteria for Voellmy friction

318 **(B) Response and (C) Changes:** We have not measured angles of internal friction and we cannot
319 back-up this statement with observations, so we think that it is appropriate to remove this sentence
320 from the manuscript because it may be confusing to readers. We edited the manuscript to clarify
321 that in fact our calibration procedure for the selection of μ does not differ significantly from that
322 proposed in the standard RAMMS model (e.g. the typical criteria for Voellmy friction). To make
323 this clear, we added a citation to Bartelt et al. (2013) and a clear statement on the calibration of
324 runout using the RAMMS model with entrainment (pages 14-15, lines 431-450).

325 **(A) Editor: Reviewer 1: Page 7, 221-222.:** please add the suggested figure

326 **(B) Response and (C) Changes:** We added the suggested figure showing the model sensitivity to
327 critical shear stress. It's now presented as the new Figure 8. The former Figure 8 is now Figure 9.
328 The (new) Figure 9 was also adapted to show the *volume growth* instead of a *bulking factor*, as
329 suggested by Reviewer 2. Please also see the more specific comments on the changes made (shown
330 above in “(C) Changes” at page 4, lines 103 ff. in this document).

331 **(A) Editor: Reviewer 2: Page 1, lines 23-24.:** provide a better reasoning for your calibration
332 procedure and highlighting also the pro and cons of the chosen procedure

333 **(B) Response and (C) Changes:** We added some additional explanation in the text (also
334 summarized in the abstract, page 1, lines 24-27) to clarify our calibration procedure, e.g. in section
335 4.1 (page 11, lines 331-333). Also, we discuss the benefits and limiting factors in the discussion
336 (section 5, page 15, lines 442-450). In the text we also refer to an extensive discussion of exactly
337 this topic (page 14, lines 440-441), which was extensively described by Frank et al., (2015).

1 **Debris flow modeling at Meretschibach and Bondasca catchment,**
2 **Switzerland: sensitivity testing of field data-based ~~erosion~~ erosion-entrainment**
3 **model**

4 Florian Frank¹, Brian W. McArdell¹, Nicole Oggier², Patrick Baer³, Marc Christen⁴ and Andreas
5 Vieli³

6 ¹ Swiss Federal Institute for Forest, Snow and Landscape Research, Birmensdorf, 8903,
7 Switzerland

8 ² wasser/schnee/lawinen, Ingenieurbüro André Burkard AG, Brig-Glis, 3900, Switzerland

9 ³ Glaciology, Geomorphodynamics & Geochronology, Department of Geography, University of
10 Zurich, Zurich, 8057, Switzerland

11 ⁴ WSL Institute for Snow and Avalanche Research SLF, Davos Dorf, 7260, Switzerland

12 *Correspondence to:* Florian Frank (florian.frank@wsl.ch)

13 **Abstract**

14 Debris flow volumes can increase due to the incorporation of sediment into the flow as a
15 consequence of channel-bed erosion along the flow path. This study describes a sensitivity analysis
16 of the recently-introduced RAMMS debris flow entrainment ~~algorithm~~ model which is intended to
17 help solve problems related to predicting the runout of debris flows. The entrainment algorithm
18 predicts the depth and rate of erosion as a function of basal shear stress based on an analysis of
19 erosion measurements at the Illgraben catchment, Switzerland (Frank et al., 2015). Starting with a
20 landslide-type initiation in the RAMMS model, the volume of entrained sediment was calculated
21 for recent well-documented debris-flow events at the Bondasca and the Meretschibach catchments,
22 Switzerland. – The sensitivity to the initial landslide volume was investigated by systematically
23 varying the initial landslide volume and comparing the resulting debris-flow volume with estimates
24 from the field sites. In both cases, the friction coefficients in the RAMMS runout model were
25 calibrated using the model where the entrainment module was (1) inactivated to find plausible
26 values for general flow properties by adjusting both coefficients (ξ and μ) and then (2) activated to
27 further refine coefficient μ which controls erosion (patterns). ~~In both cases, the friction coefficients~~
28 ~~in the RAMMS runout model were calibrated using the model where the entrainment module was~~
29 ~~inactivated.~~ The results indicate that the ~~entrainment~~ model predicts plausible erosion volumes in
30 comparison with field data. By including bulking due to entrainment in runout models, more
31 realistic runout patterns are predicted in comparison to starting the model with the entire debris-
32 flow volume (initial landslide plus entrained sediment). In particular, lateral bank overflow – not
33 observed during ~~this~~ these events – is prevented when using the sediment entrainment model, even
34 in very steep (≈ 60 – 65 %) and narrow (4–6 m) torrent channels. Predicted sediment entrainment
35 volumes are sensitive to the initial landslide volume, suggesting that the model may be useful for

36 both reconstruction of historical events as well as the modeling of scenarios as part of a hazard
37 analysis.

38 1. Introduction

39 Sediment erosion caused by debris flows ~~causes flow bulking (in our case an increase in flow mass,~~
40 ~~e.g. Iverson 1997) which strongly influences the runout strongly influences the bulking~~ behavior of
41 debris flows ~~(Iverson, 1997). The term erosion can be defined as the process of removing~~
42 ~~sediment from the channel bed while sediment entrainment describes the procedure of~~
43 ~~incorporating the eroded sediment into the debris flow.~~ The entrainment of ~~eroded~~ sediment along
44 the channel has been observed to considerably increase the volume of debris flows (~~i.e. bulking~~
45 ~~process~~) at many different locations (e.g. Hungr et al., 2005; Scheuner et al., 2009; Iverson et al.,
46 2010; Berger et al., 2010a; Berger et al., 2011; Schürch et al., 2011; Iverson et al., 2011, McCoy et
47 al., 2012; Tobler et al., 2014; Frank et al., 2015). Two recent extreme examples from the central
48 Swiss Alps in the last decade showed significant bulking along the flow path. In the Spreitgraben
49 catchment (2009-2011), the overall multi-surge event volumes increased to about 90'000 to
50 130'000 m³ – mainly due to ~~erosion-entrainment~~ along the active channel on the fan (Tobler et al.,
51 2014; Frank et al., 2015). At the Rotlauigraben catchment (2005), about 2/3 of the total volume of
52 550'000 m³ was eroded from the debris-flow fan during a multiple-surge debris-flow event
53 initiated by the failure of a glacier moraine during an intense rainfall event (Scheuner et al., 2009).
54 Therefore, the debris-flow ~~erosion-entrainment~~ and bulking process should be included in debris-
55 flow runout models to increase the accuracy of runout predictions including the overall runout
56 distance, location and amplitude of lateral bank overflow but also – importantly for hazard
57 assessment – the flow and depositional pattern on the fan (Gamma, 2000; Scheuner et al., 2009;
58 Hussin et al, 2012; Han et al., 2015; Frank et al., 2015).

59 However, models which include bulking by debris flows are relatively new and their performance
60 for practical applications has not yet been systematically investigated. Most entrainment modeling
61 studies focused on the field site where the erosion data for the underlying entrainment modeling
62 concept was collected and/or exclusively dealt with a single model application field site to test their
63 concept for entrainment modeling (e.g. Han et al., 2015; Frank et al., 2015). Herein we describe the
64 systematic application of the new RAMMS entrainment/bulking model (Frank et al., 2015) for
65 several recent events in the Swiss Alps.

66 Computational debris-flow runout models, which usually neglect ~~erosion~~~~entrainment~~, are often
67 used to assess runout distance and pattern (Crosta et al., 2003; D'Ambrosio et al., 2003; Medina et
68 al., 2008; Hungr and McDougall, 2009; Christen et al., 2012) and are therefore useful for hazard
69 analysis where predictions of flow intensity (e.g. the spatial distribution of flow depth and velocity)
70 are required (e.g. Scheuner et al., 2011). Because the debris flow process often was observed to
71 cause significant entrainment of sediment which can strongly influence the flow (e.g. Dietrich and
72 Dunne, 1978; Suwa and Okuda, 1980; Gallino and Pierson, 1984; Hungr et al., 1984; Benda, 1990;
73 Pierson et al., 1990; Meyer and Wells, 1997; Vallance and Scott, 1997; Berti et al., 1999; Cannon
74 and Reneau, 2000; Fannin and Wise, 2001; May, 2002; Wang et al., 2003; Revellino et al., 2004;

Formatted: Font: Italic

Formatted: Font: Italic

Formatted: Font: Italic

75 | Scott et al., 2005; Godt and Coe, 2007; Breien et al., 2008; Gartner et al., 2008; [Pastor et al., 2009](#);
76 | Guthrie et al., 2010; Procter et al., 2010; Berger et al., 2010; Berger et al., 2011; Schürch et al.,
77 | 2011; Iverson et al., 2011; McCoy et al., 2012; [Cascini et al., 2014](#); Tobler et al., 2014; Frank et al.,
78 | 2015), ~~the importance of~~ including entrainment and bulking debris flow runout modeling would be
79 | appropriate. Processed-based entrainment rates using algorithms which consider the material
80 | properties of the debris flow bulk (Crosta et al., 2003; D'Ambrosio et al., 2003; Medina et al.,
81 | 2008; Deubelbeiss and McArdell, 2012) as well as pre-specified entrainment rates which pre-define
82 | the absolute volume of eroded material (Beguería et al., 2009; Hungr and McDougall, 2009; Hussin
83 | et al., 2012) have been introduced in numerical runout models.

84 | Recently, we introduced an ~~erosion-entrainment~~ algorithm in the RAMMS debris flow ~~runout~~
85 | model for the assessment of debris flow ~~erosion-entrainment~~ and bulking (Frank et al., 2015). The
86 | ~~erosion-entrainment~~ algorithm uses a relation between basal shear stress and erosion ~~depth~~ based on
87 | an analysis of data from the Illgraben catchment, Switzerland (Frank et al., 2015; Berger et al.,
88 | 2011; Schürch et al., 2011). The entrainment model was used to predict the overall erosion pattern
89 | and erosion volume at the first site where it was tested, the Spreitgraben, Switzerland. However,
90 | secondary erosion processes such as bank collapse and small torrential flood events between the
91 | ~~debris-debris~~-flow events increased the uncertainty in the evaluation of the model. As a
92 | consequence, additional sensitivity tests were not made. In this study we therefore focus on testing
93 | the sensitivity of the RAMMS debris flow and entrainment model by assessing the sensitivity of
94 | total event volume (initial landslide volume plus volume of eroded sediment) to initial flow
95 | volume. This is especially important in hazard analysis where landslide scenarios are considered to
96 | trigger debris flows. For this sensitivity analysis, we evaluated two Alpine catchments with diverse
97 | topography and recent well-documented debris flows with volumes up to a few 10,000 m³: the
98 | Bondasca catchment in Southeastern Switzerland and the Meretschibach catchment in Southern
99 | Switzerland.

100 | 2. ~~Erosion-Entrainment~~ modeling study sites and available data

101 | 2.1. Meretschibach catchment, Switzerland

102 | The Meretschibach catchment is located in Southern Switzerland, adjacent to and east of the
103 | Illgraben catchment (Figure 1). The catchment area is about 9.2 km² and ranges from the summit of
104 | the Bella Tola mountain (3,025 m a.s.l.) to the confluence with a drainage channel (619 m a.s.l.)
105 | following into the Rhone River. Debris flows in the Meretschibach currently originate mainly in
106 | the Bochtür subcatchment (1.42 km² area) which is covered mostly by steep debris slopes with
107 | hillslope angles on the talus deposits of up to 60%. Patches of forest are present below the treeline
108 | (2,200 m a.s.l.) and at the margins of the catchment, and largely contiguous forest is found along
109 | both sides of the channel below an elevation of 1,600 m. The Bochtür subcatchment is underlain by

110 Triassic sericitized quartzite and white quartzites of the Bruneggjoch formation (Gabus et al. 2008).
111 The surface has several terrace-like structures have been mapped as sacking-type features (Gabus
112 et al., 2008) and are likely sources of landslides and rockfall.

113 Sediment deposits are abundant on the steep slopes of the catchment, originating from a variety of
114 mass wasting processes. Field observations of rockfall, the presence of damaged trees, and
115 unpublished records in the community forestry archives records indicate that rockfall is a dominant
116 process for generating sediment. Observations in the source area also indicate that dry ravel of
117 gravel and sand is also common in the summer months when the hillslopes are relatively dry.
118 According to the event inventory debris flows occur mainly between April and October (Szymczak
119 et al. 2010). Small debris flows start and deposit in the upper catchment, often depositing at an area
120 of lower slope located an elevation of approximately 2,000 m a.s.l. Convective storms or long
121 duration rainfall events have been observed to mobilize these sediment deposits and initiate debris
122 flows.

123 Georadar profiles on the west side of the unforested part of the Bochtür subcatchment as well a
124 airborne georadar measurements indicate that the sediment deposits are up to 5 m thick
125 (~~Fankhauser et al., 2015~~Lucas et al., 2017), although independent observations of the spatial
126 distribution of sediment thickness are not available. However extrapolation of that value to other
127 parts of the catchment must be made with caution because the profiles were made on a talus
128 deposit, which may be interpreted as a depositional area on the hillslope, that exhibits little
129 geomorphic evidence of debris-flow activity.

130 In the years 2013 and 2014 several instruments and devices were installed in the catchment. In
131 October 2013, a meteorological station was installed above the initiation zone to measure
132 precipitation, temperature and snow height. Inexpensive wildlife-observation cameras recorded
133 images every 15 minutes during daylight were positioned along the most active western channel to
134 document the changes along the active channel. A debris flow monitoring station was installed on
135 23 July 2014 (Oggier et al. 2015a). It consisted of three geophones and a radar to measure the flow
136 stage. The radar is triggered by the geophones or the meteorological station and provides detailed
137 recordings of the debris flow hydrograph at a resolution of 1 Hz.

138 During summer 2014, three debris flows occurred. Because the monitoring station was installed
139 after the first event (20 July 2014), no hydrograph data are available for this event. Precipitation
140 and hydrograph data for the ~~debris-debris~~-flow events on 28 and 29 July 2014 indicate that the
141 ~~debris-debris~~-flow event on 28 July was triggered due to convective storms with large rainfall
142 intensity (up to 3.3 mm / 10 min) while the event 29 July 2014 initiated after a few hours of steady
143 rainfall with moderate intensity (up to 1.5 mm / 10 min). The pictures from camera 4 (see Fig. 1 for
144 the location) clearly showed that the initiation of the event on July 28 took place between 19:45
145 and 20:15 (UTC +2), corresponding with the hydrograph measured at the observation station.

146 To obtain additional information about the initial volume and the spatial distribution of erosion, the
147 height models from 15 July and 28 October were compared. The digital elevation model of 17 July
148 was the result of a photogrammetry flight by swisstopo. The second digital elevation model (28
149 October) – which is a surface model (including vegetation) – was taken with a drone (Oggier et al.
150 2015b). The results indicate that the volume of the events eroded at the open debris slopes of
151 Bochtür was between 800 and 1,200 m³. Due to additional erosion downslope of the Bochtür
152 subcatchment, the total volume of the ~~debris-debris~~-flow events was between 8,000 and 10,000 m³.

153 2.2. Bondasca catchment, Switzerland

154 The Bondasca catchment in south-eastern Switzerland is a tributary to the Bergell valley (Figure 2).
155 The catchment area covers about 20.9 km². The geology is dominated by the Tertiary intrusion of
156 the Bergell granite. Originating from within the North wall of Pizzo Cengalo, a rock avalanche on
157 27 December 2011 deposited about 1.5 10⁶ m³ of sediments in the upper catchment with a runout
158 of up to two kilometers from the rock wall. The deposits are up to 17 m thick and cover an area of
159 about 0.760 km² while the hydrological sub-catchment is about 1.18 km² defined by the point
160 where the channel leaves the rock avalanche deposits at the lower end of the deposit.

161 The sudden sediment input from the rock avalanche was followed by several debris flows in the
162 summer of 2012 (5 and 14 July, 25 August, 24 September) whereof the two events in July
163 evacuated about 90'000 m³ of sediments from the rock avalanche deposit. The debris flows
164 originated mainly just below a ~~flat-shaped~~planar rock face. Some of the debris flow surges are
165 thought to have been triggered due to water accumulation at the toe of the wall causing firehose-
166 type debris flow initiation (Figure 3B and 5B) e.g. as described by Godt and Coe (2007). The slope
167 of the channel on the rock avalanche deposit varies between approx. 32° (≈ 71 %) below the flat-
168 shaped rock face and regularly decreases to 15° (≈ 33 %) at the lower end of the rock avalanche
169 deposit.

170 3. Debris-flow entrainment modeling

171 The goal of this study is to evaluate the ~~erosion-entrainment~~ algorithm implemented in the
172 RAMMS debris flow model (version 1.6.25) which has been previously described by Frank et al.
173 (2015). In particular, the sensitivity of the predicted erosion to the input parameters will be
174 investigated, and the data sets described above provide a new basis for evaluating the model. The
175 previous study (Frank et al., 2015) focused on demonstrating that more realistic runout results can
176 be achieved when including sediment entrainment and bulking into the runout model. However that
177 study also left many unanswered questions regarding the sensitivity of the model to input
178 parameters, especially the initial landslide volume, which was not possible to assess in the previous

179 study. Herein we focus on describing the sensitivity of the model to the initial landslide volume,
 180 using the two well-documented events described ~~earlier in the paper~~ *previously*.
 181 Although the RAMMS *debris* model and the *erosion-entrainment* algorithm have been published
 182 elsewhere, they will be briefly ~~described below to provide the necessary background information~~
 183 ~~for understanding the model~~. The underlying numerical formulas of shallow water equation and
 184 the Voellmy friction approach used in the RAMMS debris flow model are presented in detail in
 185 Christen et al. (2010); the ~~field-data-based-empirical~~ entrainment model is described in Frank et al.
 186 (2015).

187 3.1. Computational debris-flow model RAMMS

188 The RAMMS debris-flow model is based on 2D depth-averaged shallow water equations for
 189 granular flows in three dimensions given by the coordinates of the topographic surface of the
 190 digital elevation model in a Cartesian coordinate system (x, y, z) and at time (t) (Bartelt et al.,
 191 1999; Christen et al., 2010). The mass balance equation incorporates the field variables flow height
 192 $H(x, y, t)$ and flow velocity $U(x, y, t)$ and is given by

$$193 \quad \dot{Q}(x, y, t) = \partial_t H + \partial_x(HU_x) + \partial_y(HU_y). \quad (1)$$

194 where $\dot{Q}(x, y, t)$ describes the mass production source term and U_x and U_y represent the depth-
 195 averaged velocities in horizontal directions x and y (Christen et al., 2010). The depth-averaged
 196 momentum balance equations account for the conservation of momentum in two directions x and y :

$$197 \quad S_{g_x} - S_{f_x} = \partial_t(HU_x) + \partial_x\left(c_x HU_x^2 + g_z k_{a/p} \frac{H^2}{2}\right) + \partial_y(HU_x U_y), \quad (2)$$

$$198 \quad S_{g_y} - S_{f_y} = \partial_t(HU_y) + \partial_x(HU_x U_y) + \partial_y\left(c_y HU_y^2 + g_z k_{a/p} \frac{H^2}{2}\right). \quad (3)$$

199 where the earth pressure coefficient $k_{a/p}$ is normally set to 1 when running the standard Voellmy-
 200 Salm friction approach, c_x and c_y represent topographical coefficients determined from the digital
 201 elevation model, S_g is the effective gravitational acceleration, and S_f the frictional deceleration in
 202 directions x and y (Christen et al., 2010). The frictional deceleration S_f of the flow is determined
 203 using the Voellmy friction relation (Salm et al., 1990, and Salm, 1993) and specifies the *dry-*
 204 Coulomb *term* (friction *coefficient* μ -) scaling with the normal stress and the *viscous or turbulent*
 205 friction (*coefficient* ξ) depending on the *flow velocity* U squared (Christen et al., 2010; Christen et
 206 al., 2012; Bartelt et al., 2013):

$$207 \quad S_f = \mu \cdot \rho \cdot H g \cos(\phi) + \frac{\rho g U^2}{\xi} \quad (4)$$

Formatted: Font: Italic

Formatted: Font: Italic

208 where ρ is the mass density, g is the gravitational acceleration, ϕ is the slope angle (~~approximately~~
 209 ~~similar to the internal friction angle of the material~~), and $Hg\cos(\phi)$ is the normal stress on the
 210 overflowed surface. The tangent of the effective internal friction angle of the flow material can be
 211 defined for the resistance of the solid phase (the term containing μ) which extensively controls
 212 deceleration behavior of a slower moving flow. ~~On the other hand,~~ The resistance of the *viscous* or
 213 *turbulent* fluid phase (the term including ξ) prevails for a quicker moving flow (Bartelt et al.,
 214 2013).

Formatted: Font: Italic

Formatted: Font: Italic

215 3.2. Debris-flow entrainment model

216 The entrainment model was constructed using field data from the Illgraben catchment in
 217 Switzerland (Frank et al., 2015). The entrainment model describes the maximum erosion depth as a
 218 function of channel-bed shear stress and the vertical erosion rate of channel-bed sediment erosion.
 219 In detail, the model is based on the analysis of differential elevation models from pre- and post-
 220 event DTMs by Schürch et al. (2011b). This provides the depth of net erosion in a cell as a function
 221 of the local shear stress acting on the channel bed at the base of the flow. Similarly, the rate of
 222 erosion is constrained to be at the rate reported by Berger et al., 2011, using *in situ* erosion sensors,
 223 also at the Illgraben channel. In the analysis of Schürch et al (2011b), flow heights were determined
 224 using values interpolated between lateral levees after each event and the shear stress τ is
 225 approximated using the depth-slope product:

$$226 \quad \tau = \rho ghS \quad (5)$$

227 where ρ is the bulk mass density of the flow, h is flow height, and S is the channel slope. An
 228 approximation of the typical potential erosion depth at the Illgraben follows the 50% percentile line
 229 fit to the distribution of elevation change for four ~~debris-debris~~-flow events (Fig. 3a in Schürch et
 230 al., 2011b). The ~~erosion-entrainment~~ algorithm implemented in the RAMMS ~~entrainment-debris~~
 231 ~~flow~~ model is defined by the maximum potential erosion depth e_m and a specific erosion rate $\frac{dz}{dt}$
 232 (Frank et al., 2015). The relationship between the shear stress estimated (~~based on flow heights~~
 233 ~~observed in the field~~) and the measured erosion ~~depth~~ (Schürch et al., 2011b) is described as a
 234 linear function of shear stress using a proportionality factor $\frac{dz}{d\tau}$ (Eq. ~~26~~). The maximum potential
 235 erosion depth e_m (~~for each grid cell~~) is calculated using a critical shear stress τ_c ($= 1$ kPa) and the
 236 proportionality factor $\frac{dz}{d\tau}$ ($= 0.1$ m kPa⁻¹) as a function of basal shear stress τ (Frank et al., 2015):

$$237 \quad e_m = \begin{cases} 0 & \text{for } \tau < \tau_c \\ \frac{dz}{d\tau}(\tau - \tau_c) & \text{for } \tau \geq \tau_c \end{cases} \quad (6)$$

238 | The average rate of erosion recorded at the erosion sensor site during the Illgraben ~~debris-debris-~~
239 | flow event of 1 July 2008 (Berger et al., 2011) is used to define a specific erosion rate $\frac{dz}{dt}$.

$$240 \quad \frac{dz}{dt} = -0.025 \text{ for } e_t \leq e_m \quad (7)$$

241 | When the critical shear stress τ_c is exceeded, sediment can be entrained from the channel.
242 | Entrainment stops when the actual erosion depth e_t reaches the maximum potential erosion depth
243 | e_m (Eq. 26). Normally, the specific erosion rate is implemented using the default value $\frac{dz}{dt} =$
244 | -0.025 ms^{-1} (Eq. 37) as presented in Frank et al. (2015). However, the model also allows to
245 | account for larger or smaller ~~erosion-entrainment~~ scenarios by either doubling the rate or cutting it
246 | in half. In this study, we will use these variable erosion rates for testing the sensitivity of the model.

247 | **3.3. ~~Erosion-Entrainment~~ model setup**

248 | **3.3.1. Topographic resolution**

249 | This study focuses on the evaluation of the sensitivity of the predicted (modeled) channel-bed
250 | erosion in relation to the initial volume (e.g. initial landslide size) and the comparison of the model
251 | results and the erosion pattern observed in the field. The ability to reproduce the observed erosion
252 | patterns highly depends on a realistic representation of the channel morphology where the channel
253 | is clearly visible in the DTM (Deubelbeiss et al., 2010 and 2011; Scheuner et al., 2011; Hohermuth
254 | and Graf, 2014) and the channel dimensions (e.g. cross-sectional area) in the DTM have to be
255 | similar to what is observed in the field (e.g. Frank et al., 2015). In this study, the initial topographic
256 | data available for the Meretschibach catchment (described above) are on a square grid of 0.5 m for
257 | a channel with a width of 2 to 4 m. At the Bondasca catchment data are available on a 2 m square
258 | grid for channel varying in width from about 5 to 20 m. Although a channel width to DTM grid
259 | spacing ratio of more than 5 to 10 would probably produce more accurate results, such data are
260 | generally unavailable and the increase in the time for a simulation would be impractical.

261 | **3.3.2. ~~Erosion-Entrainment~~ model starting condition: block release and input** 262 | **hydrograph**

263 | The type of initial release mechanism, block release (e.g. landslide) or input hydrograph, can be
264 | determined based on field observations, potential model constraints and previous modeling
265 | experience using the RAMMS debris flow model (Bartelt et al., 2013). Recent debris flow
266 | modeling studies (Deubelbeiss et al., 2010; Deubelbeiss et al., 2011; Han et al., 2015) summarized
267 | that debris flows in steep channels are mostly triggered by the sudden destabilization of material
268 | originating from lateral bank collapses or dam-type deposits located within the channel itself. Han
269 | et al. (2015) concluded that a hypothetical scenario such as the breaking of a dam – which they

270 | used to start their ~~erosion-entrainment~~ model simulations – provides a stable and consistent release
271 | method. Deubelbeiss et al. (2010 and 2011), for a case study in the Swiss Alps, suggested that the
272 | block release method is most appropriate method for small to moderate initial volumes ranging
273 | from 1 m³ up to 100 m³ using the RAMMS debris flow model. The alternative release method
274 | using a discharge hydrograph seems to be more suitable for larger initial volumes (Deubelbeiss et
275 | al., 2010 and 2011) (> 100 m³) which ~~in general~~ might be plausible for the larger channel of the
276 | Bondasca catchment.

277 | The main problem with the block release is that the initial flow depth, width, or length of the initial
278 | landslide can be unrealistically large in comparison to field observations. Users have to resort to
279 | ~~such using unrealistically~~ large initial landslide volumes because most models do not allow for
280 | ~~erosion-entrainment~~ along the channel path. The total debris flow volume, typically measured in the
281 | deposition zone, is often used as the initial landslide volume, thereby implicitly ignoring the
282 | possibility that channel-bed erosion and flow bulking occur (Frank et al., 2015). The input
283 | hydrograph starting condition in RAMMS was intended to help circumvent this problem by
284 | allowing users to specify an influx of debris as a function of time at a point lower in the watershed
285 | (e.g. just above the fan apex).

286 | The block release volume is calculated by defining a specific block release height (with a precision
287 | of 1 cm ~~in this study~~) based on a pre-defined release area. The model assumes an instantaneous
288 | failure of the landslide. The initial landslide surface elevation is then set to the initial elevation of
289 | the land surface using an automatic procedure in RAMMS (the ~~“subtract release from DTM”~~
290 | option in RAMMS introduced in version 1.6.45). The main advantage of this procedure is that it
291 | prevents unrealistic lateral spreading of the initial landslide mass in comparison with a landslide
292 | “block” situated on top of the land surface.

Formatted: Font: Italic

293 | 3.3.3. Specified erosion rates

294 | As a basis for comparison of the sensitivity of the ~~erosion-entrainment~~ algorithm, we hold constant
295 | the default ~~entrainment erosion~~-model coefficients (critical shear stress τ_c , potential erosion depth
296 | as a function of basal shear stress $\frac{dz}{dt}$, erosion rate $\frac{dz}{dt}$) described above. In the previous study (Frank
297 | et al., 2015) we demonstrated that an erosion rate of $\frac{dz}{dt} = -0.025 \text{ ms}^{-1} \frac{dz}{dt} = 2.5 \text{ cm s}^{-1}$ -based on
298 | field data from the Illgraben catchment, Switzerland (Berger et al., 2011) produces plausible results
299 | for the much steeper Spreitgraben catchment. The catchments described in this paper are different
300 | in size and slope, so one might expect some variation in erosion rate. However, the ~~entrainment~~
301 | ~~erosion~~-algorithm in RAMMS allows for ~~erosion~~ rates up to $\frac{dz}{dt} = -0.05 \text{ ms}^{-1} \frac{dz}{dt} = 5.0 \text{ cm s}^{-1}$,
302 | with an option to include a shape file describing where erosion may occur e.g. to account for
303 | engineering structures such as check dams or sills, or natural features such as bedrock, where

304 significant erosion is not expected during one debris-flow event. For comparison we also used a
305 rate of $\frac{dz}{dt} = -0.0125 \text{ ms}^{-1}$ ~~$\frac{dz}{dt} = 1.25 \text{ cm s}^{-1}$~~ based on a lower rate from Berger et al. (2011).

306 4. Erosion and entrainment: observations and modeling results

307 4.1. Erosion patterns and entrainment model calibration

308 The observed erosion patterns are the basis for calibrating the RAMMS model coefficients, in
309 particular the friction coefficients ξ and μ are systematically adjusted in successive model runs,
310 until a satisfactory model result is achieved. The erosion pattern is derived by assessing the
311 difference between the digital elevation models. In both study areas, a measured erosion pattern
312 caused by one single ~~debris-debris~~-flow event is not available. We therefore focus on the spatial
313 distribution of erosion and deposition, instead of attempting to exactly predict the spatial change
314 due to the debris flow process.

315 In the Meretschibach, the change in the DTM includes the erosion due to three ~~debris-debris~~-flow
316 events which appear to have originated on an open-slope talus deposit (Figure 3A). The location of
317 the release area at the Meretschibach corresponds to the upper most visible erosion scar visible in
318 the DTM analysis and as described above includes the erosion due to three ~~debris-debris~~-flow
319 events between July 17 to October 28, 2014 (Fig. 3A). Therefore, the release area was placed
320 within the channel, where up to 2.5 meters of erosion was observed (upper end of the blue polygon
321 at about 1750 m a.s.l. in Fig. 3A.). The location is just below a bedrock step intersecting the main
322 channel at about 1800 m a.s.l. Further monitoring at the upper Bochtür subcatchment using interval
323 cameras and conducting field observations on the site itself confirmed that at least some of the
324 debris flows most likely initiated at this location.

325 We calibrated the RAMMS model using an initial block release volume of 10 m^3 which
326 corresponds to the channel depth of 1-2 m and a width of 2-4 m at this location. To keep the initial
327 volume within the channel and prevent unrealistic lateral outflow, ~~no flux boundaries were created~~
328 ~~at the lateral sides of the method of subtracting~~ the initial landslide block ~~from the elevation model~~
329 ~~was applied~~. Within the middle and lower channel sections (Fig. 3A, blue polygon), the observed
330 runout and relative erosion patterns can be best reproduced using Voellmy friction parameters $\xi =$
331 200 ms^{-2} and $\mu = 0.6$ (Fig. 3B2). ~~The parameter ξ was determined by varying it within the range~~
332 ~~proposed by the developers of the RAMMS model ($\xi = 100, 200, 400$) and inspecting the results~~
333 ~~(Bartelt et al., 2013)~~. The modeled velocities of $6\text{-}9 \text{ ms}^{-1}$ using $\xi = 200$ are plausible, although
334 independent field data are not available for comparison. The parameter combination $\xi = 200 \text{ ms}^{-2}$
335 and $\mu = 0.7$ results in overbank flow along both sides of the middle channel, which was not
336 observed in the field (Fig. 3C2). There were neither deposits ~~outside of the channel nor were levees~~
337 ~~deposited-accumulated outside of the channel~~ along this entire channel reach (Fig. 3A, blue

338 polygon). In contrast, the erosion pattern using $\xi = 200 \text{ ms}^{-2}$ and $\mu = 0.5$ resulted in an even
339 distribution of erosion along the entire channel length, which is inconsistent with the field results
340 which showed locations of deeper erosion depths (Fig. 3A). Within the normal range of the ξ
341 parameter (Bartelt et al., 2013) the differences in flow and erosion patterns were small in
342 comparison to those resulting from variations in μ , and are therefore not described herein. Hence,
343 the further model runs were conducted using the best-fit parameters $\xi = 200 \text{ ms}^{-2}$ and $\mu = 0.6$ in the
344 sensitivity analyses described in subsequent sections.

345 In the Bondasca catchment, the differential elevation model includes both the rock avalanche
346 deposit (27 December 2011) and the erosion due to one debris-flow event (5 July 5, 2012) (Fig. 5).
347 The upper end of channel erosion is located just below a planar outcrop of bedrock (Fig. 4B)
348 corresponding to the likely location debris flow initiation zone (Fig. 5C). The surface runoff
349 channels along the west side of the wall and runoff across the wall surface (Fig. 4B) converge on
350 the sediments at the bottom of the rock wall (see pictures from 2014 in Fig. 5). This scenario
351 suggests a firehose-type debris-flow initiation (e.g. Godt and Coe, 2007). Hence, this location was
352 used as the initiation area for the runout modeling.

353 The observed erosion along the main debris flow channel (Fig. 5C) – resulting from the two ~~debris~~
354 ~~debris~~-flow events in July 2012 – ~~were was~~ used to calibrate the RAMMS model within the upper
355 two thirds of the study reach (Figure 4B, brown polygon) ~~by varying the model parameters ξ and μ .~~
356 The best fit was found with the parameter combination $\xi = 400 \text{ ms}^{-2}$ and $\mu = 0.3$. However, the
357 observed elevation change also includes secondary processes such as lateral bank collapse and the
358 deposits of debris-flow snouts and levees within the channel. Channel sections where the events
359 eroded into the deposits ~~present~~ can also be identified by the stratigraphy in the field.

360 4.2. Entrainment modeling and runout patterns

361 The runout of a (landslide-type) block release of 10 m^3 , neglecting erosion (Fig. 6A) results in
362 maximum flow heights smaller than 0.5 m and the flow stops in the channel upstream of the
363 deposition zone. By contrast, including debris-flow erosion (Fig. 6B) leads to a more realistic flow
364 pattern consisting of flow within the channel reaching the deposition zone without any lateral
365 outflow. For comparison, if the total event volume ($\approx 1,555 \text{ m}^3$) is released as a landslide and the
366 debris-flow is not allowed to erode the channel (Fig. 6C), the runout shows overbank flow along
367 the upper channel reaches below the initiation area. The last scenario ~~is a typical example of how~~
368 ~~debris flow runout models are used when the total event volume is known~~ illustrates again the
369 problems associated with starting a runout model with the entire event volume assigned to the
370 initial volume. These results illustrate the ability of the runout model to better predict the erosion
371 pattern and runout if the channel-bed erosion and bulking process is included in the model.

372 4.3. Erosion model sensitivity testing

373 The results show that the total volume of eroded sediment, at both field sites, depends strongly on
 374 the initial landslide volume. At both the Meretschibach and the Bondasca catchments, there is a
 375 strong increase in the amount of sediment entrained and consequent increase in debris-flow volume
 376 (Fig. 7) for relatively small increases of the initial landslide volume. At the Meretschibach
 377 catchment, the erosion-entrainment model – using the default maximum erosion rate $\frac{dz}{dt} =$
 378 -0.025 ms^{-1} ~~$\frac{dz}{dt} = 2.5 \text{ cm s}^{-1}$~~ – shows the highest sensitivity to the total erosion volume between 2
 379 and 3 m³ of initial block release (e.g. initial landslide volume). Above 4-5 m³ of initial block
 380 volume the increase of the total erosion volume within the erosion domain remains approximately
 381 constant. The cause for the rapid increase is related to the critical shear stress in the entrainment
 382 algorithm. -Small initial landslides do not generate enough shear stress to initiate erosion, whereas
 383 larger landslides can cause erosion over the entire computational domain.

384 If we double the erosion rate to $\frac{dz}{dt} = -0.05 \text{ ms}^{-1}$ ~~$\frac{dz}{dt} = 5.0 \text{ cm s}^{-1}$~~ based on field estimates reported
 385 by Frank et al., 2015 for the Spreitgraben catchment, a similar pattern is observed in the
 386 relationship between total erosion volume as a function of initial release volume. However the
 387 erosion volumes are 3 to 5 times larger than the ones resulting from the default erosion rate at the
 388 same initial release volume. In contrast, implementing only half the default maximum erosion rate
 389 ~~$(\frac{dz}{dt} = -0.0125 \text{ ms}^{-1})$ ~~$(\frac{dz}{dt} = 1.25 \text{ cm s}^{-1})$~~~~ for low erosion-entrainment scenarios decreases the
 390 sensitivity to initial volume in an analogous manner.

391 Similar trends in total erosion volume as a function of initial block release (landslide) volume are
 392 observed at the Bondasca catchment. However, the model only starts to predict significant erosion
 393 volumes for block releases exceeding 20 m³, and the progressive increase in total erosion volume
 394 as a function of initial block release volume is somewhat less steep. For the default erosion rate
 395 ~~$\frac{dz}{dt} = -0.025 \text{ ms}^{-1}$ ~~$\frac{dz}{dt} = 2.5 \text{ cm s}^{-1}$~~~~ (Frank et al., 2015), total erosion volumes increase most
 396 strongly between initial volumes of 20 to 100 m³. The topography at the Bondasca catchment is
 397 somewhat less steep and more variable, which may help explain these differences. Doubling the
 398 default erosion rate at the Bondasca catchment results in the onset of erosion for initial volumes
 399 between 20 and 30 m³. When reducing the default erosion rate to half of the default value, the
 400 erosion model depicts a somewhat less sensitive reaction of the erosion-entrainment model than
 401 using the default rate.

402 Further assessment of the relation of the total erosion volumes depending on the initial volumes can
 403 be made by calculating a bulking factor growth rate (Hungr et al., 2005). We call it volume growth
 404 (VG) because we address an overall ratio for a specific channel section instead of a classic “yield
 405 rate” per running meter (Hungr et al., 2005): - The bulking factor BF is the ratio between the total
 406 erosion volume V_{ero} to the initial volume V_{ini} :

407 ~~$BFVG = V_{final}/V_{ini} = (V_{ini} + V_{ero})/V_{ini}$~~ (8)

408 The volume growth (VG) is the ratio between the final debris flow volume V_{final} (consisting of the
409 initial volume V_{ini} and the erosion volume V_{ero}) to the initial volume V_{ini} . We analysed the
410 development of the volume growth (VG) to assess the sensitivity to various model parameters such
411 as critical shear stress τ_c (Fig. 8) as well as erosion rate $\frac{dz}{dt}$ and initial volumes V_{ini} (Fig. 9).

412 5. Discussion

413 The total erosion volumes observed in the sensitivity tests (Fig. 7) indicate a strong sensitivity to
414 block release volume (initial landslide volume) over a relatively narrow range of block release
415 volumes. This result is based on the assumption that the entire landslide fails instantaneously and
416 not progressively as a sequence of smaller landslides over a longer period of time. Information on
417 the style of initial landslide failure are not available for either field site, therefore we focus the
418 discussion on other factors related to the runout modeling. One striking difference between the two
419 field sites is that the size of the block release necessary to cause significant erosion is an order of
420 magnitude larger at the Bondasca site. The channel cross-sectional area where the flow travels and
421 therefore where the ~~erosion-entrainment~~ model is active is different at the two field sites. The
422 Meretschibach is substantially steeper (50 to 65% vs. 15 to 35%). This results in larger shear
423 stresses at the Meretschibach for the same initial landslide thickness, because the shear-stress varies
424 as the product of initial release thickness, flow density, and channel slope. Other factors such as
425 differences in channel-bed roughness may also be important, however the Voellmy friction relation
426 within RAMMS does not explicitly consider channel-bed roughness.

427 In the RAMMS debris flow model, the development of the flow properties is controlled by the
428 Voellmy friction parameters ξ and μ (described in section 3.1) where ξ is the dominant control over
429 the flow velocities when the flow is moving rapidly and μ controls the runout distance (Bartelt et
430 al., 2013). The ξ parameter was found in this study to have a relatively small influence over the
431 flow behavior in comparison with the Coulomb friction term μ . However, a calibration of the
432 parameter ξ using an approximate discharge (block release volume or hydrograph implementation)
433 and as observed at a particular channel section can help determine the most plausible ξ value
434 within the ranges proposed by the developers of the RAMMS model ($\xi = 100, 200, 400$) (Bartelt et
435 al., 2013). The RAMMS manual (Bartelt et al., 2013) suggests using the tangent of the fan slope as
436 first estimate to determine μ . As described in the calibration procedure (section 3.24.1), this
437 corresponds to relative erosion patterns ~~measured-determined~~ by differential DTM analysis. Hence,
438 we conclude that the tangent of the channel slope can be used as a first approach to define
439 parameter μ also for the ~~erosion-entrainment~~ model when applying to channel sections which
440 exhibit a roughly constant channel slope, which-This was also found to be useful by Frank et al.
441 (2015) in the first application of the model.

442 For some field studies, applying this two-stage calibration method (inactive vs. active entrainment
443 model) will benefit model users who previously conducted RAMMS runout modeling studies
444 without entrainment. They can enhance their existing calibration procedure of parameter ξ and μ
445 by mainly refining on parameter μ to reflect a documented, relative erosion pattern when activating
446 the entrainment model. In that sense, this method might be primarily limited by the potential lack
447 of field data (flow heights, discharge, erosion patterns) which were available in this study.
448 However, more case studies are needed before we are able to draw any general conclusions
449 regarding potential benefits and limits of this enhanced methodology for the RAMMS entrainment
450 model application.

451 Morphological-In general, morphological effects influence the erosional behavior of the field data
452 based ~~erosion-entrainment~~ model. The Bondasca channel is more variable in width and planform
453 direction compared to the comparably uniform and straight Meretschibach channel. This difference
454 will cause larger spatial variability in shear stress at Bondasca channel and therefore the channel
455 will have a more variable onset of debris flow erosion along the length of the channel. In the
456 Bondasca catchment, the channel where erosion takes place is significantly wider (4-10 m) than in
457 the Meretschibach (1-3 m). On the one hand, the flow can laterally spread more often in Bondasca
458 than in the Meretschibach, thereby locally reducing flow height, shear stresses and maximum
459 potential erosion depth. On the other hand, once the critical shear stress is exceeded, the potential
460 erosion depth tends to increase more rapidly in a narrow channel such as in the Meretschibach
461 channel.

462 Other studies have addressed the spatio-temporal variation of bed entrainment interplaying with
463 debris flow rheology (Cuomo et al., 2014; Cuomo et al., 2016). In RAMMS, we do not adjust the
464 Voellmy friction coefficients as a function of flow properties because data to support the
465 implementation of bed entrainment-flow properties interplay is not available for the catchments
466 addressed herein (Meretschibach and Bondasca).

467 Another difference between the Meretschibach and the Bondasca channels is that the Bondasca
468 channel bed has a rougher surface with more scours holes, and larger blocks within the channel
469 which are similar in size to the nominal width of the channel. The model does not consider local
470 variations in erodibility due to the presence of large blocks, so local scour patterns in the field
471 around the large blocks are not present in the model results. Prancevic and Lamb⁷ (2015a)
472 suggested that in rough mountain channels the large particles can be interlocked and hence more
473 stable. In contrast, local concentration of the flow between such large blocks may cause locally
474 very large shear stresses and corresponding large erosion rates. However, we do not have enough
475 information on the mobility of the large blocks, so this question cannot be addressed in more detail
476 herein.

477 The current version of the RAMMS debris flow model with ~~erosion-entrainment~~ (version 1.6.45)
478 does not adjust the elevation of the bed when erosion occurs. The erosion can be subtracted from

479 the initial DTM as a post-processing step within the user interface, e.g. for modeling subsequent
480 surges. This issue was discussed at length by Frank et al (2015), and it can potentially complicate
481 the interpretation of erosion patterns resulting from multiple debris flows. Insufficient field data are
482 available to help constrain the events described herein.

483 ~~Further assessment of the relation of the total erosion volumes depending on the initial volumes can~~
484 ~~be made by calculating a bulking factor. The bulking factor BF is the ratio between the total~~
485 ~~erosion volume V_{ero} to the initial volume V_{ini} :~~

$$486 \quad \text{BF} = V_{\text{ero}} / V_{\text{ini}} \quad (9)$$

487 ~~For the sensitivity assessment of volume growth (VG) to the critical shear stress τ_c , we selected the~~
488 ~~Meretschibach catchment because it has a simple single-channel morphology and therefore serves~~
489 ~~as a clear case for illustration (Fig. 8). Because the erosive channel reach addressed in our study~~
490 ~~shows steep slopes reaching 50 to 65 %, the resulting shear stresses are very high – even for very~~
491 ~~low flow heights and small initial volumes (1-10 m³). This leads to a high model susceptibility to~~
492 ~~erosion (volumes) and volume growth when $\tau_c = 0$ kPa which results in scenarios of a few cubic~~
493 ~~meters of initial volumes eroding some 1,000 to more than 10,000 cubic meters (Fig. 8). However~~
494 ~~the initial landslides observed at the Meretschibach were larger in volume, suggesting that a critical~~
495 ~~shear stress is appropriate. Small debris flows do not necessarily erode the channel bed, which has~~
496 ~~been observed in the field e.g. at the Illgraben (Schürch et al., 2011; Berger et al., 2010). The~~
497 ~~presence of a critical shear stress in steep channels is also supported by investigations of~~
498 ~~entrainment in torrential sediment transport (Lamb et al., 2008), although we are not aware of any~~
499 ~~systematic investigations of the critical shear stress for entrainment by landslides or debris flows.~~

500 ~~The results show that when exceeding $\tau_c = 0.5$ kPa, the volume growth remains steady within a~~
501 ~~value range of 20 to 60 for middle to larger initial volumes (≥ 10 -50 m³). Smaller initial volumes (\leq~~
502 ~~5-10 m³) show much more variation, i.e. are more sensitive to the critical shear stress. We conclude~~
503 ~~that a value of $\tau_c = 1$ kPa produces plausible results and we use that value for the other sensitivity~~
504 ~~tests in this study. However it may be possible to constrain this value at other field sites if small~~
505 ~~non-erosive debris flows can be identified and used to better constrain τ_c . The critical shear stress~~
506 ~~of $\tau_c = 1$ kPa used herein will be applied for further sensitivity analysis.~~

507 ~~The sensitivity to initial landslide volume is apparent at the Meretschibach. Using the default~~
508 ~~erosion rate and an initial volume of 3 m³, a volume growth of ≈ 200 is reached. A maximum of~~
509 ~~VG = 300 is observed for an initial release volume of 4 m³. At the Meretschibach channel, the~~
510 ~~bulking factor is when the erosion model using the default erosion rate and an initial volume of 3~~
511 ~~m³ (Fig. 8). The BF reaches a peak $\text{BF}_p \approx 300$ at a release volume of 4 m³. It then drops to a $\text{BF} \cdot \text{VG}$~~
512 ~~≈ 30 for an initial volume of 100 m³. The model simulations using the doubled default erosion rate~~
513 ~~show a volume growth bulking factor peak $\text{VG}_p \cdot \text{BF}_p \approx 1,800$ for an initial release volume of 2 m³;~~

514 half the default erosion rate shifts this peak to 50 m^3 for the initial volume but the corresponding
515 ~~peak bulking factor~~volume growth peak drops significantly down to $VG_p \approx 14$.

516 The behavior of the ~~bulking factor~~volume growth for the default erosion rate at the Bondasca
517 catchment is relatively smooth when compared to that at the Meretschibach. But comparing erosion
518 patterns as modeled using 10 vs. 20 m³ as the initial volume in the Bondasca case e.g., we observed
519 that the model run using 20 m³ is large enough that part of the flow enters a secondary channel. The
520 volume of the flow, then divided among two channels, causes a reduction in flow depth and a
521 consequent decrease in shear stress, resulting in smaller erosion depths and therefore smaller
522 erosion volumes – leading to lower volume growth approaching a value of 1 ($VG \approx 1.2$) for $V_{ini} =$
523 20 m³ compared to $VG \approx 3$ for $V_{ini} = 10 \text{ m}^3$. When using an initial volume of 10 m³ then the flow
524 remains entirely in the main channel. This may provide an explanation for the dip in the Bondasca
525 volume growth between $V_{ini} = 10 \text{ m}^3$ and $V_{ini} = 20 \text{ m}^3$.

526 A volume growth peak ~~bulking factor~~ can be identified ~~somewhere~~ between 200 and 500 m^3 but the
527 value is lower in comparison ($\approx 4-10-12.5$) for the default erosion rate. The doubled rate leads to a
528 volume growth peak ~~peak bulking factor~~ $VG_p BF_p$ of ≈ 700 at a release volume of 30 m^3 . That is
529 ~~still~~ large compared to examples in the literature ($VG BF$ from 10 to 50 reported by Berti et al.,
530 1999 and Vandine and Bovis, 2002).

531 Nevertheless, a several hundred fold increase of the debris flow volume due to bulking is plausible
532 for extreme ~~erosion-entrainment~~ cases. Larger erosion rates might be expected for pyroclastic
533 deposits (not present in the catchments described herein) or due to the presence of very recent rock
534 avalanche deposits which may contain firm-ice-debris mixtures (e.g. Spreitgraben, Tobler et al.,
535 2014; Frank et al., 2015). Such highly erosive events represent an inherent feedback in the
536 entrainment process whereby a rapid (e.g. double) erosion rate results in a more rapid increase in
537 flow depth leading to larger shear stresses and then to even larger potential erosion depths. This can
538 potentially explain the very rapid growth of debris flows, which is has been observed in some
539 natural field cases (e.g. Spreitgraben, Tobler et al., 2014; Frank et al., 2015) and also in laboratory
540 experiments involving realistic debris-flow sediments (e.g. video documentation of experiments at
541 the USGS Debris-flow flume 1992-2006, Logan & Iverson, 2007).

542 In addition, ~~I~~ large erodibilities may be expected at the Bondasca catchment because the rock
543 avalanche event occurred during winter and may have contained significant amount of snow.
544 However, ~~d~~Due to the very long ($\approx 4 \text{ km}$) and flat ($\approx 15\%$) channel section in the middle segment
545 of the Bondasca catchment, the estimated deposition volumes ($\approx 40,000 \text{ m}^3$) above the inlet of the
546 Bondasca river in the central valley are highly influenced by further erosional and depositional
547 processes along the channel.

548 6. Conclusion

549 Debris-flow runout predictions can be improved when considering the increase in flow volume
550 along the flow path. Using a recently-introduced empirical [erosion-entrainment](#) algorithm within
551 the RAMMS 2D runout model (Frank et al., 2015) we illustrate that runout patterns at the
552 Meretschibach and Bondasca catchments, in Switzerland, can be accurately modeled. When
553 calibrated with field data, the model produces more realistic runout patterns compared to
554 simulations which do not consider entrainment and bulking. In particular, we could show that even
555 in very steep ($\approx 60\text{--}65\%$) and narrow (4–6 m) torrent channels, lateral overflow – not observed in
556 the field case – is prevented when applying the entrainment model. However the model results can
557 be quite sensitive to the volume of the initial block release in the model which corresponds to the
558 initial landslide volume. The predicted erosion volumes are sensitive to the initial debris flow
559 volume, with [bulking-factors](#)[volume growth values](#) approaching 2000 predicted by the model,
560 depending on the scenario considered. However, the results are also sensitive to slope angle and
561 channel morphology. The two field sites differ substantially: the Meretschibach catchment is very
562 steep with a straight and narrow channel, whereas the Bondasca channel is less steep ~~but~~[and](#)
563 morphologically more complex, yet the calibration procedure is the same as for the standard
564 RAMMS model which does not include the entrainment process. The overall method presented
565 herein is useful for case studies where sufficient data are available to constrain the model results.
566 However, more case studies have to be conducted to develop a more comprehensive
567 recommendation for modeling the runout of erosive debris flows in natural terrain.

568 **Acknowledgements**

569 This project was partially supported by the CCES-TRAMM project. We are grateful to Christian
570 Huggel for helpful discussions and comments. We thank Martin Keiser of Amt für Wald und
571 Naturgefahren of Canton Graubünden for providing elevation data for the Bondasca catchment and
572 Ruedi Bösch, WSL, for the elevation data at the Meretschibach catchment. [The debris-flow
573 observations at the Meretschibach were partially financed by SNF Project 200021_144362/1 as
574 well as related contributions by the Canton of Valais and the community of Agarn. We are grateful
575 to Sarah Springmann \(ETH\) and Andrew Kos \(ETH and Terrasense LTD\) for insightful
576 discussions on the stability of the Meretschibach catchment.](#)

577 **References**

- 578 ~~Beguería, S., Van Asch, Th. W. J., Malet, J. P., and Gröndahl, S.: A GIS-based numerical model~~
579 ~~for simulating the kinematics of mud and debris flows over complex terrain, Nat. Hazards Earth~~
580 ~~Syst. Sci., 9, 1897–1909, doi:10.5194/nhess-9-1897-2009, 2009.~~
- 581 Bartelt, P., Buehler, Y., Christen, M., Deubelbeiss, Y., Graf, C., and McArdell, B. W.: RAMMS –
582 rapid mass movement simulation, A modeling system for debris flows in research and practice,
583 user manual v1.5, debris flow, manuscript update: 31 January 2013, WSL Institute for Snow
584 and Avalanche Research SLF, available at:
585 http://ramms.slf.ch/ramms/downloads/RAMMS_DBF_Manual.pdf (last access: 27 February
586 2015), 2013.
- 587 ~~Beguería, S., Van Asch, Th. W. J., Malet, J.-P., and Gröndahl, S.: A GIS-based numerical model~~
588 ~~for simulating the kinematics of mud and debris flows over complex terrain, Nat. Hazards Earth~~
589 ~~Syst. Sci., 9, 1897–1909, doi:10.5194/nhess-9-1897-2009, 2009.~~
- 590 Benda, L.: The influence of debris flows on channels and valley floors in the Oregon Coast Range,
591 USA. Earth Surf. Proc. Landf. 15, 457-466, 1990.
- 592 ~~Berger, C., McArdell, B. W., Fritschi, B. and Schlunegger, F.: A novel method for measuring the~~
593 ~~timing of bed erosion during debris flows and floods, Water Resour. Res., 46, W02502,~~
594 ~~doi:10.1029/2009WR007993, 2010.~~
- 595 Berger, C., McArdell, B.W., and Schlunegger, F.: Sediment transfer patterns at the Illgraben
596 catchment, Switzerland: Implications for the time scales of debris flow activities,
597 Geomorphology, 125, 421–432, 2010.
- 598 Berger, C., McArdell, B. W., and Schlunegger, F.: Direct measurement of channel erosion by
599 debris flows, Illgraben, Switzerland, J. Geophys. Res., 116, F01002,
600 doi:10.1029/2010JF001722, 2011.
- 601 Berti, M.; Genevois, R.; Simoni, A. and Tecca, P.R.: Field observations of a debris flow event in
602 the Dolomites. Geomorphology, 29:265–274, 1999.
- 603 Breien, H., De Blasio, F. V., Elverhøi, A & Høeg, K. Erosion and morphology of a debris flow
604 caused by a glacial lake outburst flood, western Norway. Landslides 5, 271-280, 2008.
- 605 Cannon, S. H. and Reneau S. L.: Conditions for generation of fire-related debris flows, Capulin
606 Canyon, New Mexico, Earth Surf. Processes Landforms, 25(10), 1103–1121, 2000.
- 607 ~~Cascini, L., Cuomo, S., Pastor, M., Sorbino, G. and Piciullo, L.: SPH run-out modelling of~~
608 ~~channelised landslides of the flow type. Geomorphology Volume 214, 1 June 2014, 502–513,~~
609 ~~<http://dx.doi.org/10.1016/j.geomorph.2014.02.031>, 2014.~~
- 610 Christen, M., Kowalski, J., and Bartelt, P.: RAMMS: Numerical simulation of dense snow
611 avalanches in three-dimensional terrain, Cold Reg. Sci. Technol., 63, 1–14, 2010.
- 612 Christen, M., Bühler, Y., Bartelt, P., Leine, R., Glover, J., Schweizer, A., Graf, C., McArdell, B.
613 W., Gerber, W., Deubelbeiss, Y., Feistl, T., and Volkwein, A.: Integral hazard management

614 using a unified software environment: numerical simulation tool “RAMMS” for gravitational
615 natural hazards, edited by: Koboltschnig, G., Hübl, J., Braun, J., 12th Congress
616 INTERPRAEVENT, 23–26 April 2012 Grenoble, France, Proceedings, Vol. 1, Klagenfurt,
617 International Research Society INTERPRAEVENT, 77–86, 2012.

618 Crosta, G. B., Imposimato, S., and Roddeman, D. G.: Numerical modelling of large landslides
619 stability and runout, *Nat. Hazards Earth Syst. Sci.*, 3, 523–538, doi:10.5194/nhess-3-523-2003,
620 2003.

621 [Cuomo, S., Pastor, M., Capobianco, V. and Cascini, L.: Modelling the space–time evolution of bed](#)
622 [entrainment for flow-like landslides. *Engineering Geology* Volume 212, 30 September 2016,](#)
623 [10–20, <http://dx.doi.org/10.1016/j.enggeo.2016.07.011>, 2016.](#)

624 [Cuomo, S., Pastor, M., Cascini, L., Castorino, G.C.: Interplay of rheology and entrainment in](#)
625 [debris avalanches: a numerical study. *Can. Geotech. J.* 1–15, \[2013-0387, 2014.\]\(http://dx.doi.org/10.1139/cgj-

626 <a href=\)](#)

627 D’Ambrosio, D., Di Gregorio, S., and Iovine, G.: Simulating debris flows through a hexagonal
628 cellular automata model: SCIDDICA S3-hex, *Nat. Hazards Earth Syst. Sci.*, 3, 545–559,
629 doi:10.5194/nhess-3-545-2003, 2003.

630 Deubelbeiss, Y.; Graf C.; McArdell, B.; Bartelt, P.: Numerical modeling of debris flows – Case
631 study at Dorfbach, Randa (VS), Swiss Geoscience Meeting. Fribourg, 2010.

632 Deubelbeiss, Y.; Graf, C.; McArdell, B.; Bartelt, P. Numerical modeling of debris flows – Case
633 study at Dorfbach, Randa (Valais, Switzerland). *Geophysical Research Abstracts* Vol. 13,
634 EGU2011-5681, EGU General Assembly 2011, Vienna, 2011.

635 Deubelbeiss, Y. and McArdell, B. W.: Dynamic modelling of debris-flow erosion and deposition
636 with application to the USGS debris flow flume experiments, *Geophys. Res. Abstr.* 14,
637 EGU2012-7906, 2012.

638 Dietrich, W. E., and Dunne, T.: Sediment budget for a small catchment in mountainous terrain, *Z.*
639 *Geomorphology*, 29, 191–206, 1978.

640 Fannin, R. J. and Wise, M. P.: An empirical_statistical model for debris flow travel distance. *Can.*
641 *Geotech. J.* 38, 982-994, 2001.

642 [Lucas, D. R., Fankhauser, K. and Springman S. M.: Application of geotechnical and geophysical](#)
643 [field measurements in an active alpine environment. *Engineering Geology*, Volume 219, 9](#)
644 [March 2017, Pages 32–51, <http://dx.doi.org/10.1016/j.enggeo.2016.11.018>, 2017.](#)

645 [Fankhauser F., Lucas Guzman D. R., Oggier N., Maurer H., Springman S. M. 2015. Seasonal](#)
646 [Response and Characterization of a Scree Slope and Active Debris Flow Catchment Using](#)
647 [Multiple Geophysical Techniques: The case of the Meretschibach Catchment, Switzerland.](#)
648 [Geophysical Research Abstracts Vol. 17, EGU2015-PREVIEW, EGU General Assembly 2015,](#)
649 [2015.](#)

650 Frank, F., McArdell, B. W., Huggel, C., and Vieli, A.: The importance of entrainment and bulking
651 on debris flow runout modeling: examples from the Swiss Alps, *Nat. Hazards Earth Syst. Sci.*,
652 15, 2569-2583, doi:10.5194/nhess-15-2569-2015, 2015.

653 Frank, F., McArdell, B. W., Huggel, C., and Vieli, A.: Sediment input and debris flow system
654 activity cycles - an analysis of the development in different catchments in Switzerland. In prep.

655 Gabus, J. H., Weidmann, M., Bugnon, P.-C., Burri, M., Sartori, M., and Marthaler, M.: Geological
656 map of Sierre, LK 1278, sheet 111, scale 1:25,000, in *Geological Atlas of Switzerland*, Swiss
657 Geol. Surv., Bern, Switzerland, 2008.

658 Gallino, G. L., and Pierson, T. C.: The 1980 Polallie Creek debris flow and subsequent dam-break
659 flood, East Fork Hood River Basin, Oregon, U.S. Geol. Surv. Open File Rep., 84-578, 37 pp.,
660 1984.

661 Gamma, P.: "dfwalk" Ein Murgang-Simulationsmodell zur Gefahrenzonierung. Institute of
662 Geography, University of Berne. *Geographica Bernensia* G66 (only available in German), 2000.

663 Gartner, J. E., Cannon, S. H., Santi, P. M. and Dewolfe, V. G.: Empirical models to predict the
664 volumes of debris flows generated by recently burned basins in the western U.S.,
665 *Geomorphology*, 96(3-4), 339-354, 2008.

666 Godt, Jonathan W. and Coe, Jeffrey A.: Alpine debris flows triggered by a 28 July 1999
667 thunderstorm in the central Front Range, Colorado, *Geomorphology*, Volume 84, Issues 1-2,
668 Pages 80-97, ISSN 0169-555X, <http://dx.doi.org/10.1016/j.geomorph.2006.07.009>. 15 February
669 2007.

670 Guthrie, R. H., Hockin, A., Colquhoun, L., Nagy, T., Evans, S.G. and Ayles, C.: An examination
671 of controls on debris flow mobility: Evidence from coastal British Columbia. *Geomorphology*
672 114, 601-613, 2010.

673 Han, Zheng; Chen, Guangqi; Li, Yange; Tang, Chuan; Xu, Linrong; He, Yi; Huang, Xun; Wang,
674 Wei: Numerical simulation of debris-flow behavior incorporating a dynamic method for
675 estimating the entrainment, *Engineering Geology*, Volume 190, Pages 52-64, ISSN 0013-7952,
676 14 May 2015, available at: <http://dx.doi.org/10.1016/j.enggeo.2015.02.009> (last access: 10
677 February 2016), 2015.

678 Hohermuth, B. and Graf, C.: Einsatz numerischer Murgangsimulationen am Beispiel des integralen
679 Schutzkonzepts Plattenbach Vitznau. *Wasser Energ. Luft* 106, 4: 285-290, available at:
680 <http://www.wsl.ch/wsl/info/mitarbeitende/grafc/pdf/14138.pdf> (last access: 10 February 2016),
681 2014.

682 Hungr, O., McDougall, S. and Bovis, M.: Entrainment of material by debris flows, in *Debris-Flow*
683 *Hazards and Related Phenomena*, edited by M. Jakob and O. Hungr, pp. 135-158, Springer,
684 New York, 2005.

685 Hungr, O., Morgan, G. C. and Kellerhals, R.: Quantitative analysis of debris torrent hazards for
686 design of remedial measures, *Can. Geotech. J.*, 21(4), 663-677, 1984.

687 Hungr, O. and McDougall, S.: Two numerical models for landslide dynamic analysis, Comput.
688 Geosci., 5, 978–992, 2009.

689 Hussin, H. Y., Quan Luna, B., van Westen, C. J., Christen, M., Malet, J.-P., and van Asch, Th. W.
690 J.: Parameterization of a numerical 2-D debris flow model with entrainment: a case study of the
691 Faucon catchment, Southern French Alps, Nat. Hazards Earth Syst. Sci., 12, 3075–3090,
692 doi:10.5194/nhess-12-3075-2012, 2012.

693 Iverson, R. M.: The Physics of Debris Flows: IN: Reviews of Geophysics, 35, 3, August 1997, p.
694 245.296, published by Geophysical Union, Paper # 97RG00426, 1997.

695 Iverson, R.M., Reid, M.E., Logan, M., LaHusen, R.G., Godt, J.W. and Griswold, J.G.: Positive
696 feedback and momentum growth during debris-flow entrainment of wet bed sediment. Nature
697 Geoscience v. 4, no. 2, p. 116-121. doi: 10.1038/NGEO1040, 2011.

698 Iverson, R.M., Reid, M.E., Logan, M., LaHusen, R.G., Godt, J.W., and Griswold, J.G.: Positive
699 feedback and momentum growth during debris-flow entrainment of wet bed sediment. Nature
700 Geoscience v. 4, no. 2, p. 116-121. doi: 10.1038/NGEO1040, 2011.

701 [Lamb, M. P., Dietrich, W. E. and Venditti, J. G.: Is the critical Shields stress for incipient sediment](#)
702 [motion dependent on channel-bed slope?, J. Geophys. Res., 113, F02008,](#)
703 [doi:10.1029/2007JF000831, 2008.](#)

704 [Logan, M. and Iverson, R.M.: Video documentation of experiments at the USGS Debris-flow](#)
705 [flume 1992-2006, U.S. Geological Survey Open-File Report 2007-1315, 2007.](#)

706 May, C. L.: Debris flows through different forest age classes in the Central Oregon Coast Range, J.
707 Am. Water Resour. Assoc., 38(4), 1097-1113, 2002.

708 McCoy, S. W., Kean, J. W., Coe, J. A., Tucker, G. E., Staley, D. M. and Wasklewicz, T. A.:
709 Sediment entrainment by debris flows: In situ measurements from the headwaters of a steep
710 catchment, J. Geophys. Res., 117, F03016, doi:10.1029/2011JF002278, 2012.

711 Medina, V., Hürlimann, M., and Bateman, A.: Application of FLATModel a 2-D finite volume
712 code, to debris flows in the northeastern part of the Iberian Peninsula, Landslides, 5, 127–142,
713 2008.

714 Meyer, G. A., and Wells, S. G.: Fire-related sedimentation events on alluvial fans, Yellowstone
715 National Park, USA, J. Sediment. Res., 67(5), 776-791, 1997.

716 Oggier, N. and McArdeall, B. W.: Ereignisanalyse - Murgangereignisse Meretschibach 20./28./29.
717 Juli 2014. [WSL](#) Birmensdorf, 21. Januar 2015, ([unpublished report, only available](#) in German),
718 2015a.

719 Oggier, N. and Bösch, R.: Zwischenbericht, Drohnenflug Meretschibach 28. Oktober 2014, [WSL](#)
720 Birmensdorf, 26. Februar 2015, ([unpublished report, only available](#) in German), 2015b.

721 [Pastor, M., Haddad, B., Sorbino, G., Cuomo, S. and Drempetic, V.: A depth-integrated, coupled](#)
722 [SPH model for flow-like landslides and related phenomena. Int. J. Numer. Anal. Meth.](#)
723 [Geomech., 33: 143–172. doi:10.1002/nag.705, 2009.](#)

Formatted: references

Formatted: English (U.S.)

724 Pierson, T. C., Janda, R. J., Thouret, J-C. and Borrero, C. A.: Perturbation and melting of snow and
725 ice by the 13 November 1985 eruption of Nevado del Ruiz, Colombia, and consequent
726 mobilization, flow and deposition of lahars. *J. Volcanol. Geotherm. Res.* 41, 17-66, 1990.

727 Prancevic, J. P., and Lamb, M. P.: Particle friction angles in steep mountain channels, *J. Geophys.*
728 *Res. Earth Surf.*, 120, doi:10.1002/2014JF003286, 2015a.

729 Prancevic, J. P., and M. P. Lamb: Unraveling bed slope from relative roughness in initial sediment
730 motion, *J. Geophys. Res. Earth Surf.*, 120, doi:10.1002/2014JF003323, 2015b.

731 Procter, J., Cronin, S. J., Fuller, I. C., Lube, G. and Manville, V.: Quantifying the geomorphic
732 impacts of a lake-breakout lahar, Mount Ruapehu, New Zealand, *Geology*, 38(1), 67-70, 2010.

733 Revellino, P., Hungr, O., Guadagno, F. M. and Evans, S. G.: Velocity and runout simulation of
734 destructive debris flows and debris avalanches in pyroclastic deposits, Campania region, Italy,
735 *Environ. Geol.*, 45(3), 295-311, 2004.

736 Scheingross, J. S., Winchell, E.W., Lamb, M. P. and Dietrich, W. E.: Influence of bed patchiness,
737 slope, grain hiding, and form drag on gravel mobilization in very steep streams, *J. Geophys.*
738 *Res. Earth Surf.*, 118, 982-1001, doi:10.1002/jgrf.20067, 2013.

739 Scheuner, T., Keusen, H., McArdell, B. W., and Huggel, C.: Murgangmodellierung mit dynamisch-
740 physikalischem und GIS-basiertem Fließmodell, Fallbeispiel Rotlauigraben, Guttannen, August
741 2005, *Wasser Energie Luft*, 101: 15-21 (only available in German), 2009.

742 Scheuner, T., Schwab, S., and McArdell, B. W.: Application of a two-dimensional numerical
743 model in risk and hazard assessment in Switzerland, in 5th DFHM, Padua, Italy, 2011.

744 Schürch, P., Densmore, A. L., Rosser, N. J., and McArdell, B. W.: Dynamic controls on erosion
745 and deposition on debris-flow fans, *Geology*, 39, 827-830, 2011.

746 Scott, K. M., Vallance, J. W., Kerle, N., Macias, J. L. Strauch, W. and Devoli, G.: Catastrophic
747 precipitation-triggered lahar at Casita volcano, Nicaragua: Occurrence, bulking and
748 transformation, *Earth Surf. Processes Landforms*, 30(1), 59-79, doi:10.1002/esp.1127, 2005.

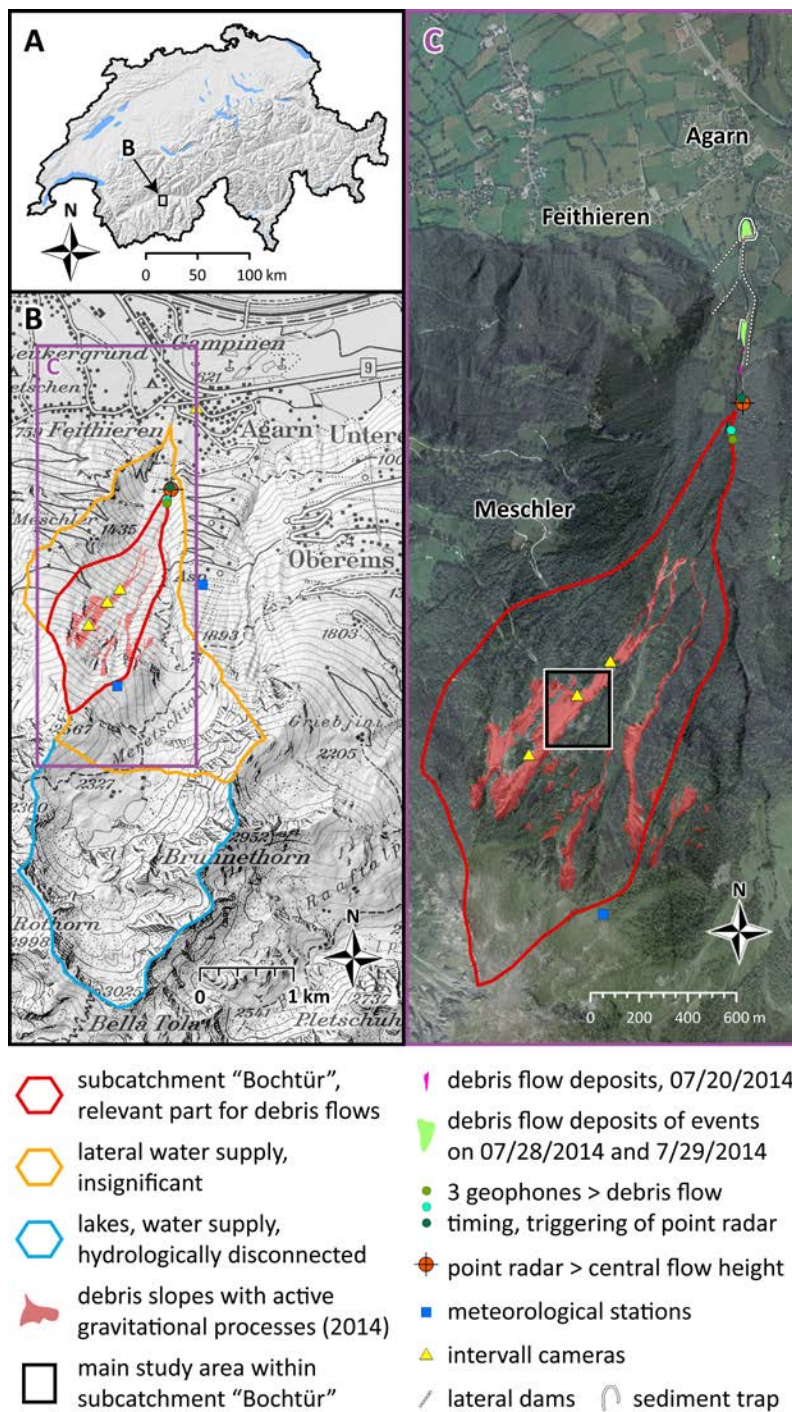
749 Suwa, H., and Okuda, S.: Dissection of valleys by debris flow, *Z. Geomorphology*, 35, 164-182,
750 1980.

751 Szymczak, S., Bollschweiler, M., Stoffel, M. and Dikau, R.: Debris-flow activity and snow
752 avalanches in a steep watershed of Valais Alps (Switzerland): Dendrogeomorphic event
753 reconstruction and identification of triggers. *Geomorphology* 116, 107-114, 2010.

754 Tobler, D., Kull, I., Jacquemart, M., and Haehlen, N.: Hazard Management in a Debris Flow
755 Affected Area: Case Study from Spreitgraben, Switzerland, *Landslide Science for a Safer*
756 *Geoenvironment*, 3, 25-30, doi:10.1007/978-3-319-04996-0_5, 2014.

757 Vallance, J. W. and Scott, K. M.: The Osceola Mudflow from Mount Rainier: Sedimentology and
758 hazard implications of a huge clay-rich debris flow, *Geol. Soc. Am. Bull.*, 109(2), 143-163,
759 1997.

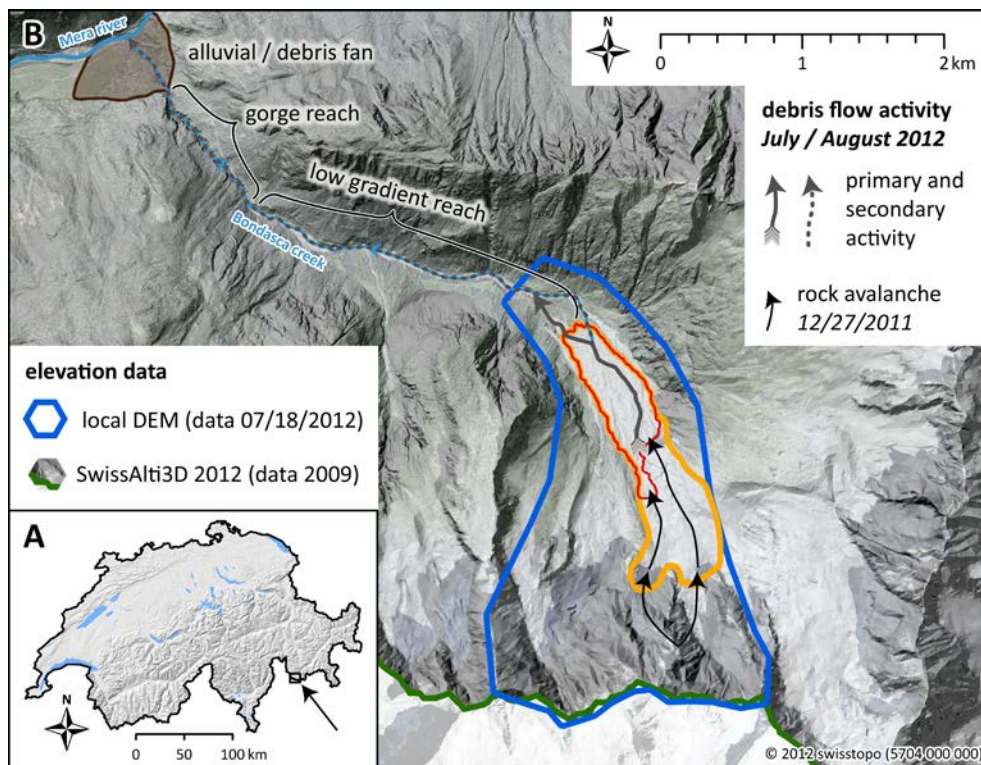
760 Vandine, D.F. and Bovis M.: History and goals of Canadian debris-flow research, a review. Nat
761 Hazards 26:69–82, 2002.
762 Wang, G., Sassa, K. and Fukuoka, H.: Downslope volume enlargement of a debris
763 ~~slide-debris~~slide-debris flow in the 1999 Hiroshima, Japan, rainstorm. Eng. Geol. 69, 309-330,
764 2003.



765

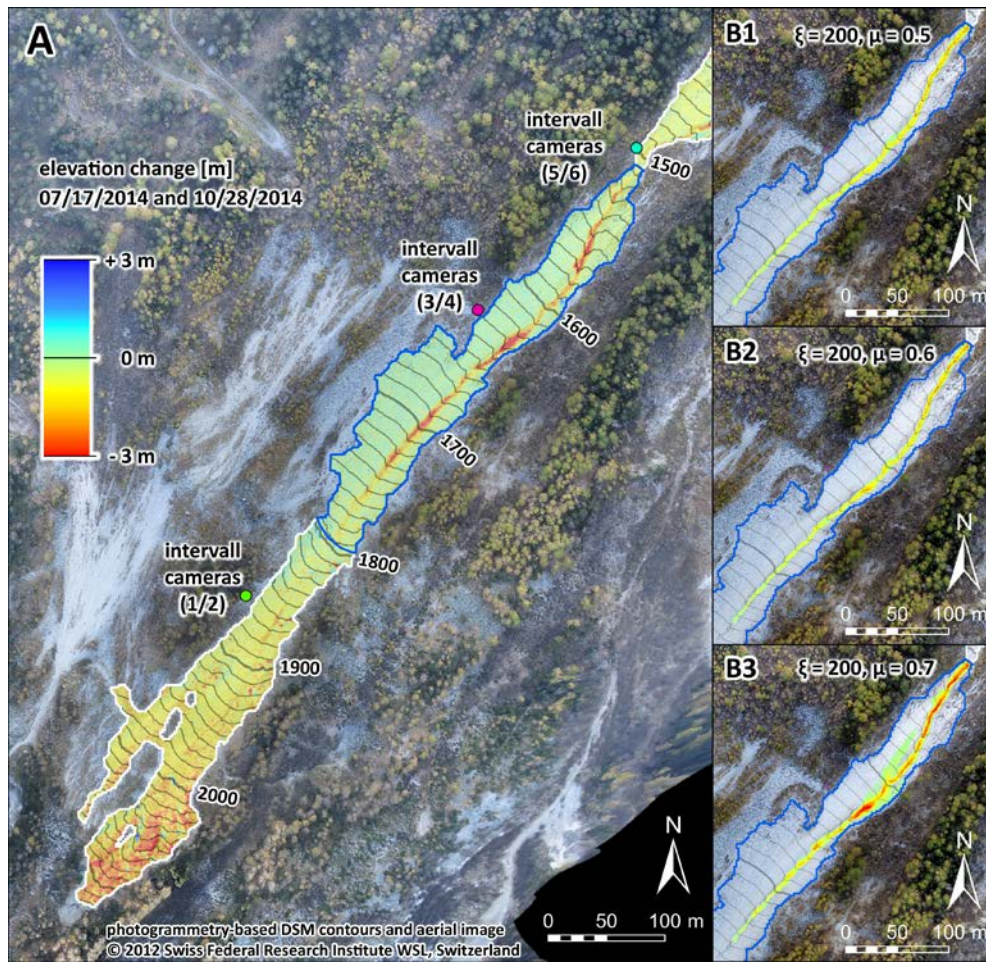
766 **Figure 1.** A. Location of the Meretschibach catchment in Southern Switzerland. B. Subcatchments
 767 of the Meretschibach and locations of the instrumentation site and data available for the erosion
 768 model analyses C. Initiation zone of the July 2014 events and camera positions. The main study

769 channel reach for the model testing is located in the middle part of “Bochtür” (black-white
770 retangle), swissimage©2014, swisstopo (5704 000 000) (2014).



771

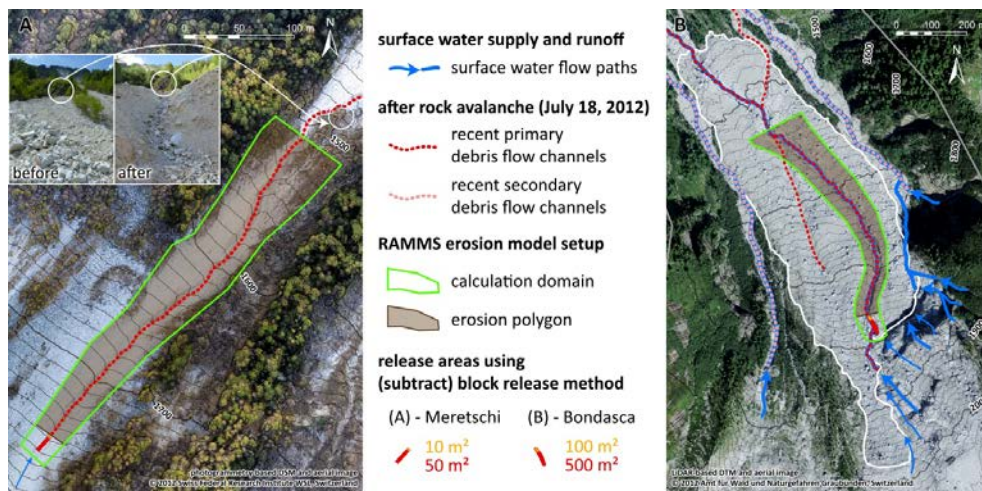
772 **Figure 2. A.** Location of the Bondasca catchment in south-eastern Switzerland close to the border
773 to Italy. **B.** Perimeter of the 27 December 2011 rock avalanche deposit, including the main
774 deposition area (yellow polygon) and the deposits lower-elevation deposits which have been
775 partially exposed to erosion by debris flows in 2012 (red polygon). The 2012 post-event digital
776 elevation model (lidar, blue polygon) is from 18 July 2012 (data courtesy of the Amt für Wald,
777 Canton Graubünden). Pre-event digital elevation model (lidar) for 2009 is from the SwissAlti3D
778 (version 2012) data set from swisstopo, ©2012, swisstopo (5704 000 000) . The grey solid arrow
779 indicates the main debris-flow channel formed in 2012.



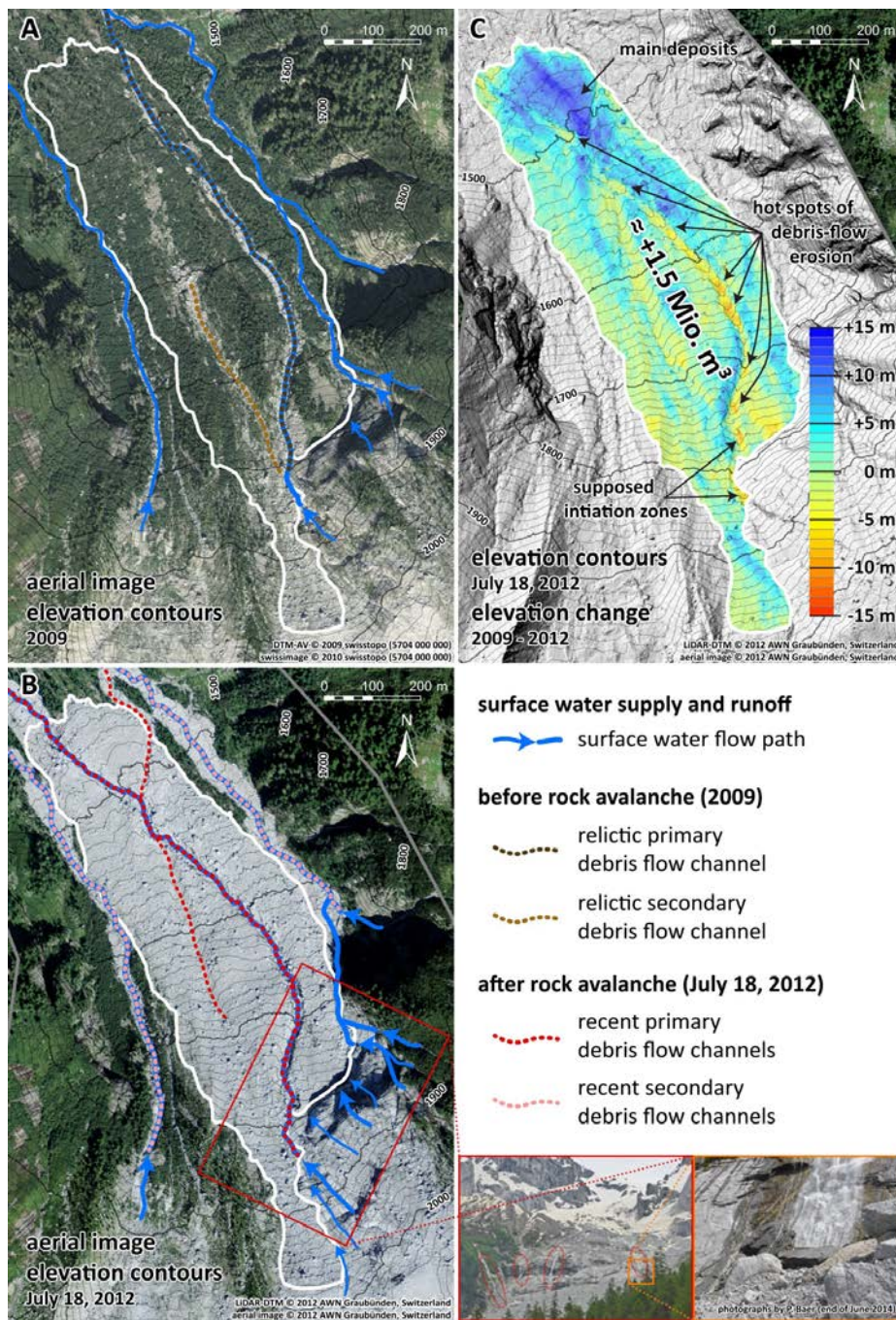
780

781 **Figure 3.** Calibration of modelled erosion patterns (**B1 to B3**) to the observed erosion depths (**A**) in
 782 the upper open debris slopes of the “Bochtür” catchment (Meretschibach) by varying values for the
 783 friction parameter μ . The blue polygon demarks the area where a differential DTM is available.

784

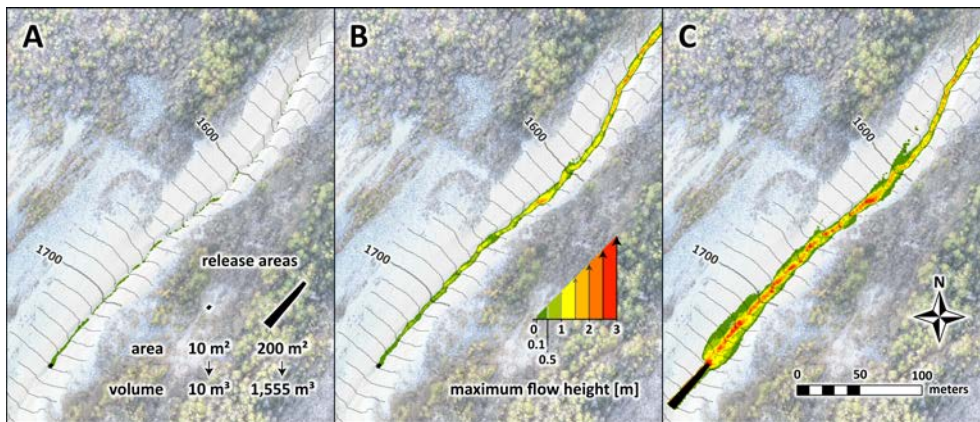


785 **Figure 4.** Erosion model configuration for the model simulations showing the initial block release
786 areas in the Meretschibach catchment (A) and the Bondasca catchment, Switzerland (B). The
787 hillslope is erodible within the brown shaded polygon.



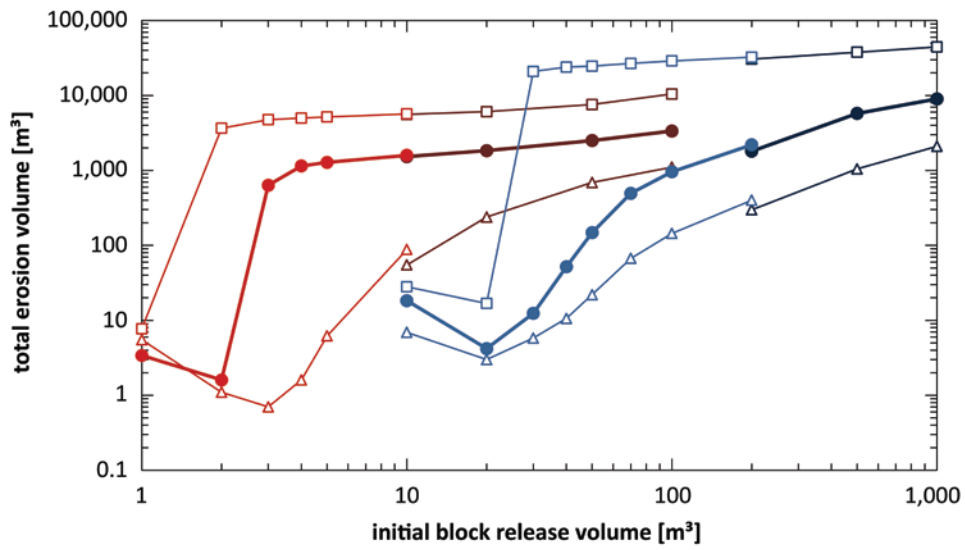
788

789 **Figure 5.** Overview of rock avalanche deposits, subsequently formed debris flow channels, and the
 790 resulting overall elevation change in the Bondasca catchment (A, B). The elevation change map
 791 2009 to 2012 (C) includes both the rock avalanche ($\approx 1.5 \text{ Mio m}^3$ on 27 Dec. 2011) and the first
 792 two debris-debris-flow events (5 and 14 July 2012).



793

794 **Figure 6.** Comparison of runout patterns at “Bochtür” in the Meretschi catchment. The debris flow
 795 modeling is conducted using a (subtract) block release volume of (A) 10 m^3 and no-entrainment
 796 modeling, of (B) 10 m^3 and entrainment modeling as well as a total (subtract) block release volume
 797 of (C) $1,555 \text{ m}^3$ (sum of release and eroded volume from (B)) and no-entrainment modeling.

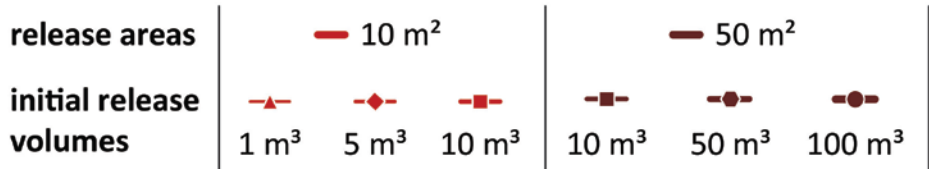
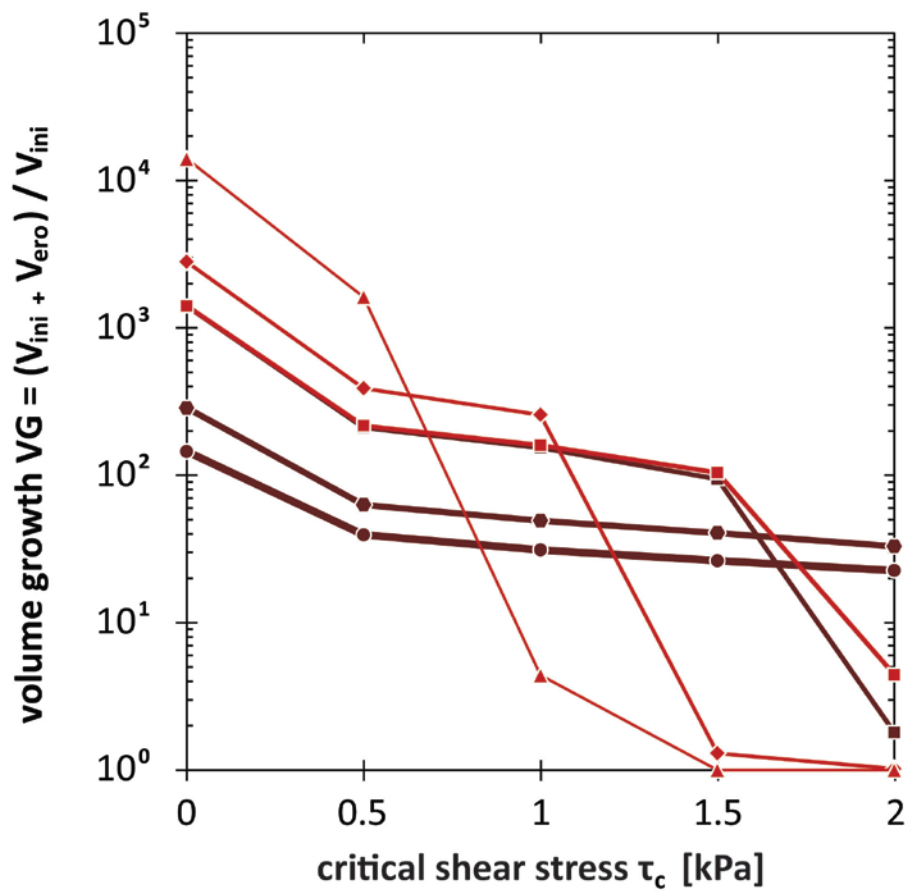


	Meretschi	Bondasca
calibrated parameters	$\xi = 200 \text{ m}^2\text{s}^{-1}, \mu = 0.60$	$\xi = 400 \text{ m}^2\text{s}^{-1}, \mu = 0.30$
release areas	— 10 m ² — 50 m ²	— 100 m ² — 500 m ²
erosion rates (Frank et al., 2015)	△ 1.25 cm s ⁻¹ ● 2.5 cm s ⁻¹	□ 5.0 cm s ⁻¹

798

799 **Figure 7.** Sensitivity of modeled erosion volume to initial block release volume in the
 800 Meretschibach and in the Bondasca catchments.

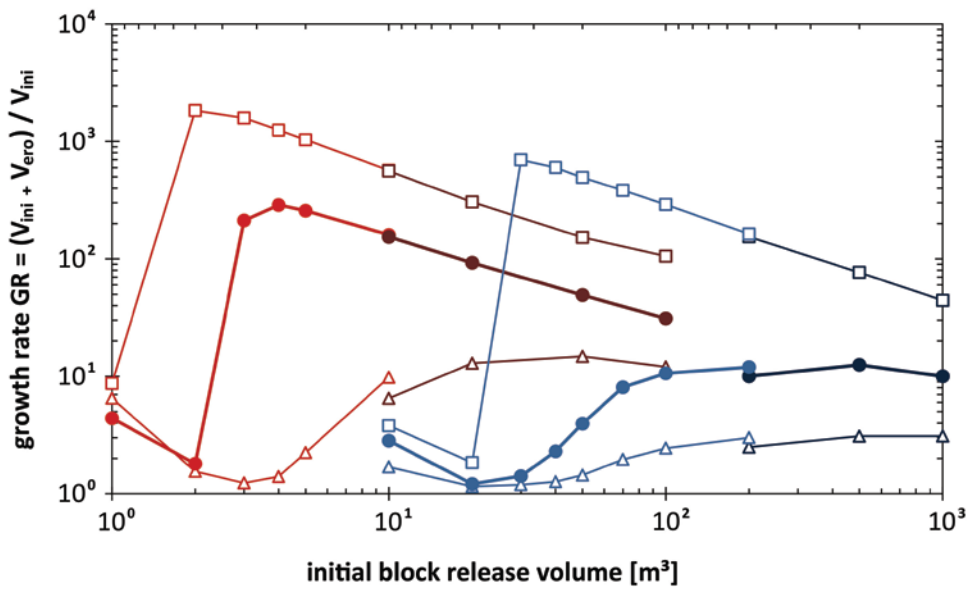
Formatted: English (U.S.)



801

802 **Figure 8.** Sensitivity of the volume growth $VG = (V_{ini} + V_{ero}) / V_{ini}$ to the critical shear stress τ_c
 803 depending on 5 different initial (block release) volumes V_{ini} as set up based on two release areas in
 804 the Meretschibach catchment.

Formatted: English (U.S.)



	Meretschi	Bondasca
calibrated parameters	$\xi = 200 \text{ m}^2\text{s}^{-1}, \mu = 0.60$	$\xi = 400 \text{ m}^2\text{s}^{-1}, \mu = 0.30$
release areas	— 10 m ² — 50 m ²	— 100 m ² — 500 m ²
erosion rates (Frank et al., 2015)	△ 1.25 cm s ⁻¹ ● 2.5 cm s ⁻¹	□ 5.0 cm s ⁻¹

805

806 **Figure 89.** The ~~bulking factor BF~~ volume growth $VG = (V_{ini} + V_{ero}) / V_{ini}$ consisting of the modeled
 807 ~~sum of total the~~ erosion volume V_{ero} [m³] ~~to and~~ initial block release volume V_{ini} [m³] ~~per initial~~
 808 ~~block release volume~~ V_{ini} [m³] and addressing three different erosion rates ~~in for~~ the Meretschibach
 809 and Bondasca catchments.